Abnormal loading on two types of short span bridge

Abnormal Loading on Two Types of Short Span Bridge

Charges exceptionnelles sur deux types de ponts de faible portée

Ausnahmebelastung auf zwei Brückentypen mit kurzen Spannweiten

R. E. ROWE

M.A., A.M.I.C.E., Great Britain

Introduction

In Great Britain many highway bridges have spans of from 20 to 60 ft., this being particularly true of bridges carrying modern motorways. It would thus appear that there is a need for a general type of bridge for such spans which could carry both the Ministry of Transport standard and abnormal loading and could be built easily, quickly, and economically.

For a number of years the Cement and Concrete Association has been studying the design and behaviour of various types of bridge subjected to abnormal loading (1—4) and the more recent work has included a study of a type of bridge to meet the above requirements; the type of bridge considered was a box-section bridge employing a considerable amount of precast concrete. This type of bridge was considered because

a) it possesses the optimum load distribution characteristics for a given area of concrete section;

b) it can be conveniently constructed using precast units with virtually no shuttering needed on site;

c) it can be made monolithic by means of transverse prestress; and

d) it can be constructed quickly and economically.

Two model bridges of this type have been tested to investigate the validity of the methods of design and construction.

Another possible type of bridge for short spans subjected to abnormal loading is the composite slab bridge; this type comprises precast prestressed inverted T-beams with an in situ concrete fill. The main disadvantage in the

past has been that it was thought necessary to prestress such slabs transversely to ensure adequate distribution of load; this prestress is both difficult to place and expensive. It would seem logical to replace the transverse prestress by mild steel reinforcement and to accept a lesser degree of load distribution. To investigate this possibility, three composite slab bridges have been tested to determine the deterioration in the distribution properties and the applicability of ultimate load methods for the design of the transverse reinforcement.

Box-Section Bridge [5]

Details of Bridge

The bridge was approximately a one-third scale model of an actual highway bridge with a carriageway 22 ft. wide and two footpaths each 5 ft. wide; the available space in the laboratory limited the span to 14 ft. The design was governed by the Ministry of Transport abnormal loading, as is usual for spans of between 20 and 60 ft.

The design incorporated three main units: a precast prestressed inverted T-beam; a precast diaphragm; a precast reinforced slab. Originally it was intended to cast each beam in one operation on a pre-tensioning bed but, unfortunately, the pre-tensioning bed was at that time in constant use for another series of tests. Hence it was necessary to manufacture the beams in a number of units, joint the units to form beams, and post-tension them. The beam units and diaphragms had mild-steel hair-pins, inserted after casting and vibrated into position, on the faces which were to be jointed with in situ concrete. The mesh reinforcement in the slabs projected beyond the edges to be jointed. Apart from the hairpins there was no shear reinforcement in the webs of the T-beams.

For the transverse prestress it was found necessary to use an eccentric prestress to provide a balanced design, i. e. the longitudinal and transverse working loads for the Ministry of Transport abnormal loading were equal.

Materials

The concrete used in the manufacture of the individual units was a 1 : 1.4 : 2.8 mix using ordinary Portland cement, Feltham sand and a $^3/_{16}$—$^3/_8$ in. Mount Sorrel granite aggregate; the water/cement ratio was 0.4. Three 4 in. cubes were cast from each batch of concrete mixed; these were tested at ages of 7 days, 14 days, and at the time of the final test to failure. The average strengths were: 6,100 lb./in.^{2} at 7 days; 7,500 lb./in.^{2} at 14 days; 11,100 lb./in.^{2} at the time of the final test.

Construction

As the units for each beam became available they were set up on a level bed and 0.276 in. diameter wires were threaded through the ducts enabling the joints to be made with dry packed mortar. When the joints were mature the prestress was applied; 0.2 in. diameter wires were threaded through the ducts and stressed with Gifford-Udall jacks. When completed each beam was placed in position on the abutments, the supports consisting of a 1 in. mild steel roller at one end with a similar roller fixed in position at the other. Each beam was individually supported and great care taken to ensure that the ducts for the transverse prestressing wires were in alinement with those in the other beams.

When the six inverted T-beams were in position the longitudinal joints between the beams were packed with mortar. Scaffold planks were shored into position to provide shuttering for the joints and to ensure that no load came on to them (the joints between the main beams were $1/2$ in. wide). The next stage was the insertion of all the diaphragms relevant to the six main beams. The joints between diaphragms and beams were $1/4$ in. wide and these needed special care; the diaphragms were placed on $1/2$ in. diameter mild steel bars threaded through the transverse stressing ducts, and each joint was packed from both sides. Fig. 1 illustrates this stage in the construction.

The edge beams were placed in position, jointed to the rest of the bridge, and the remaining diaphragms were then placed and jointed.

The top slabs were placed in position on the beams and diaphragms. Each
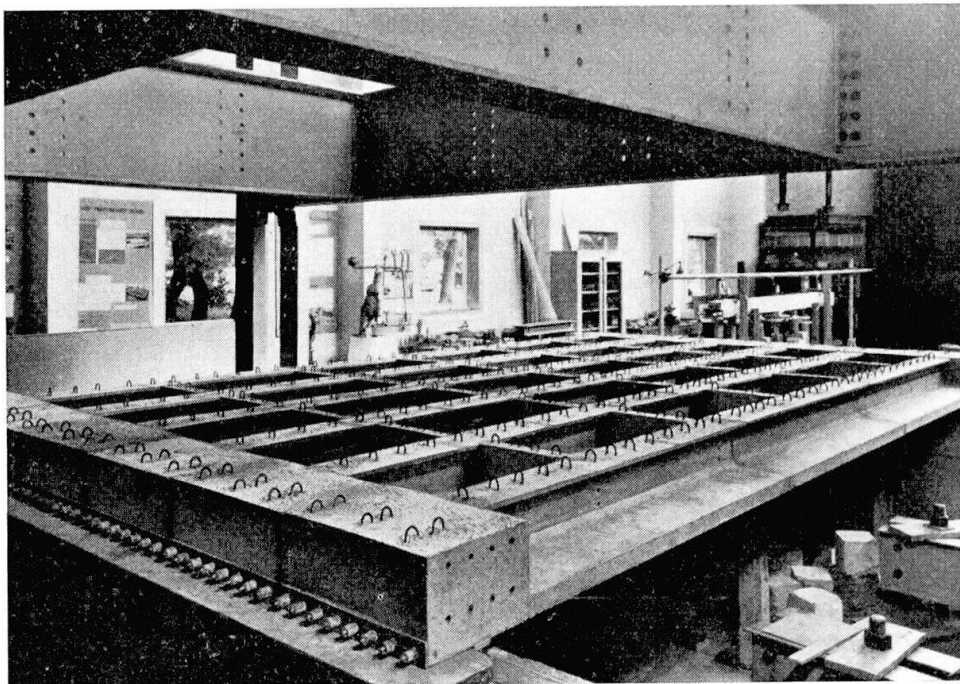
Fig. 1. Box-Section Bridge — Six Main Beams and Diaphragms After Jointing.

slab was bedded down on mortar of average thickness $^3/_8$ in., this thickness varying where necessary to give a plane top surface to the bridge. Edge shuttering was erected to enable the final jointing concrete to be placed. This concrete was of the same mix as was used for the individual units and was placed by hand. Finally the 0.276 in. diameter transverse stressing wires were threaded through the ducts and stressed by Gifford-Udall jacks. The end blocks were stressed first, then the central diaphragm and then the remaining diaphragms.

Control Beam

To enable the value of Young's modulus for the concrete to be determined at various ages, an additional inverted T-beam was produced. This was set up as a simply supported beam over a 14 ft. span and loaded at two points symmetrically placed at 42 in. centres. Deflexion measurements were obtained at the mid- and quarter-span sections and from these a value of Young's modulus was deduced: the mean value during the tests was 4.5×10^6 lb./in^2. The control beam was also used to check the accuracy of 1 in. electrical resistance foil gauges on a concrete with a maximum aggregate size of $^3/_8$ in. Readings from foil gauges were compared with those obtained using a demountable mechanical strain gauge with an 8 in. gauge length. The agreement between the readings of the two types of gauge was excellent, as is shown in Fig. 2.

Fig. 2. Box-Section Bridge — Comparison of Strain Readings From Electrical Resistance and Mechanical Strain Gauges on Control Beam.

Analysis and Discussion of Results

Deflexions

Details of the various loadings used in the tests are given in Table 1; the numbers assigned to the various loadings will be used throughout this section of the paper. For ea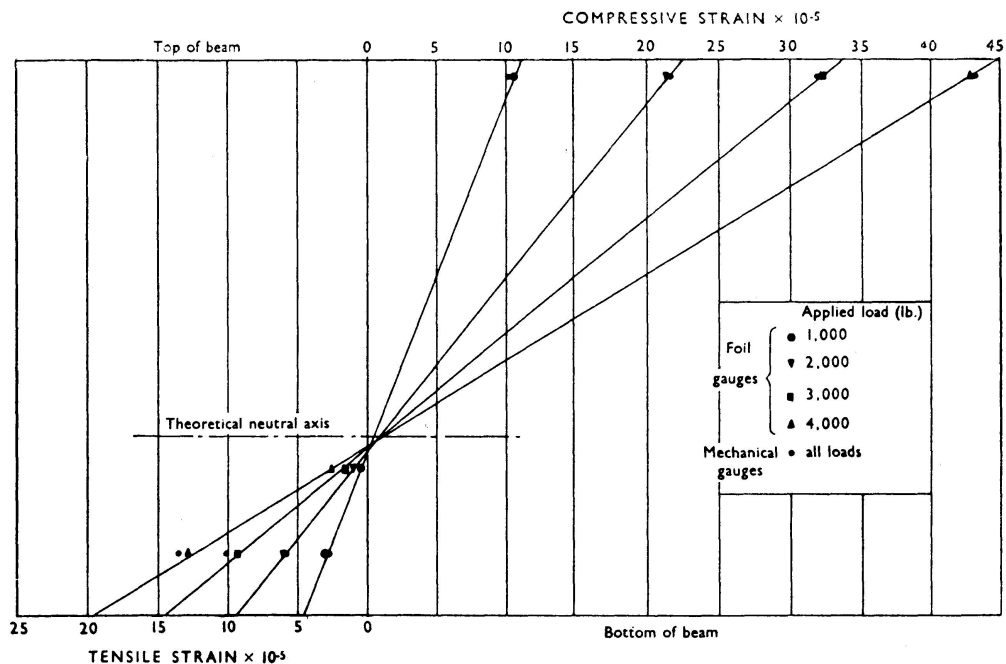ch loading, deflexion profiles were obtained; from the profiles the "mean" deflexion was derived by the application of Simpson's rule. Hence the distribution coefficients were obtained from the actual deflexions and the measured "mean" deflexion, due allowance being made for the effect of settlement. Fig. 3 compares the theoretical and experimental distribution coefficient profiles for the various loadings. For all loadings the agreement between theoretical and experimental values of the distribution coefficient is very good in the region of the load, even for the concentrated loading No. 7 where the discrepancy is about 10 %. At the edges of the bridge the discrepancies increase, being greatest at the edge remote from the load. The curves given in Fig. 8 for loading No. 3, 4 and 6 demonstrate the accuracy to be expected in assessing deflexions under the Ministry of Transport abnormal load when a load distribution analysis is assumed. The close agreement also justified the relaxation method used in the determination of the torsional parameter for the bridge [4].

For the design loading, i. e. loading No. 6, the deflexion profiles at various load stages are shown in Fig. 4; in this Figure the magnitude of the corrections for settlement may be seen. It is interesting to observe the gradual breakdown of the distribution properties of the bridge, indicated by the changing form

Table 1. Box-Section Bridge — Details of Various Loadings Used on Bridge

Loading No.	Transverse position of wheels measured from edge of bridge (in.)				Maximum load applied (tons)
1		56 $\frac{1}{4}$	68 $\frac{1}{4}$		8
2		32 $\frac{1}{4}$	44 $\frac{1}{4}$		8
3	32 $\frac{1}{4}$	44 $\frac{1}{4}$	56 $\frac{1}{4}$	68 $\frac{1}{4}$	12
4	8 $\frac{1}{4}$	20 $\frac{1}{4}$	32 $\frac{1}{4}$	44 $\frac{1}{4}$	12
5	44 $\frac{1}{4}$	56 $\frac{1}{4}$	68 $\frac{1}{4}$	80 $\frac{1}{4}$	15
6	20 $\frac{1}{4}$	32 $\frac{1}{4}$	44 $\frac{1}{4}$	56 $\frac{1}{4}$	20
7		38			20
8		93 $\frac{3}{4}$	117 $\frac{3}{4}$		18

For loadings No. 1—7 wheels were symmetrically placed at 2 ft. centres about transverse centre-line of bridge. For loading No. 8 both wheels were on transverse centre-line.

of the curves, at loads in excess of the theoretical working load of 12.7 tons. Between 15 tons and the maximum load of 20 tons, cracking of the edge beam and first inverted T-beam caused these members to deflect equally and a corresponding increase occurred in the loads sustained by the remaining members of the bridge. Fig. 5 shows the load-deflexion curves for the more heavily loaded edge beam under loading No. 6. This loading was applied three times to determine the zero-tension or working load of the bridge. The discontinuity in the elastic region was due to the presence of shrinkage cracks in the jointing concrete between the top slabs. These cracks were only in the transverse direction as the transverse prestress had closed them in the longitudinal direction. This resulted in an increase in the stiffness of the bridge at a load corresponding to the closing of these shrinkage cracks. This behaviour

Fig. 3. Box-Section Bridge — Comparison of Theoretical and Experimental Distribution Coefficient Profiles for Deflexions for Various Loadings.

was identical for all beams but did not appear to effect the distribution pro-
perties of the bridge. The slight difference in slope of the load-deflexion curves
for the three loadings was due to incomplete recovery of the bridge between
loadings. The experimental working load appears to be 13 tons and the load
at which cracks formed to be 15 tons. This cracking load corresponds to a
tensile strength of 150 lb./in.^{2} in the jointed beams.
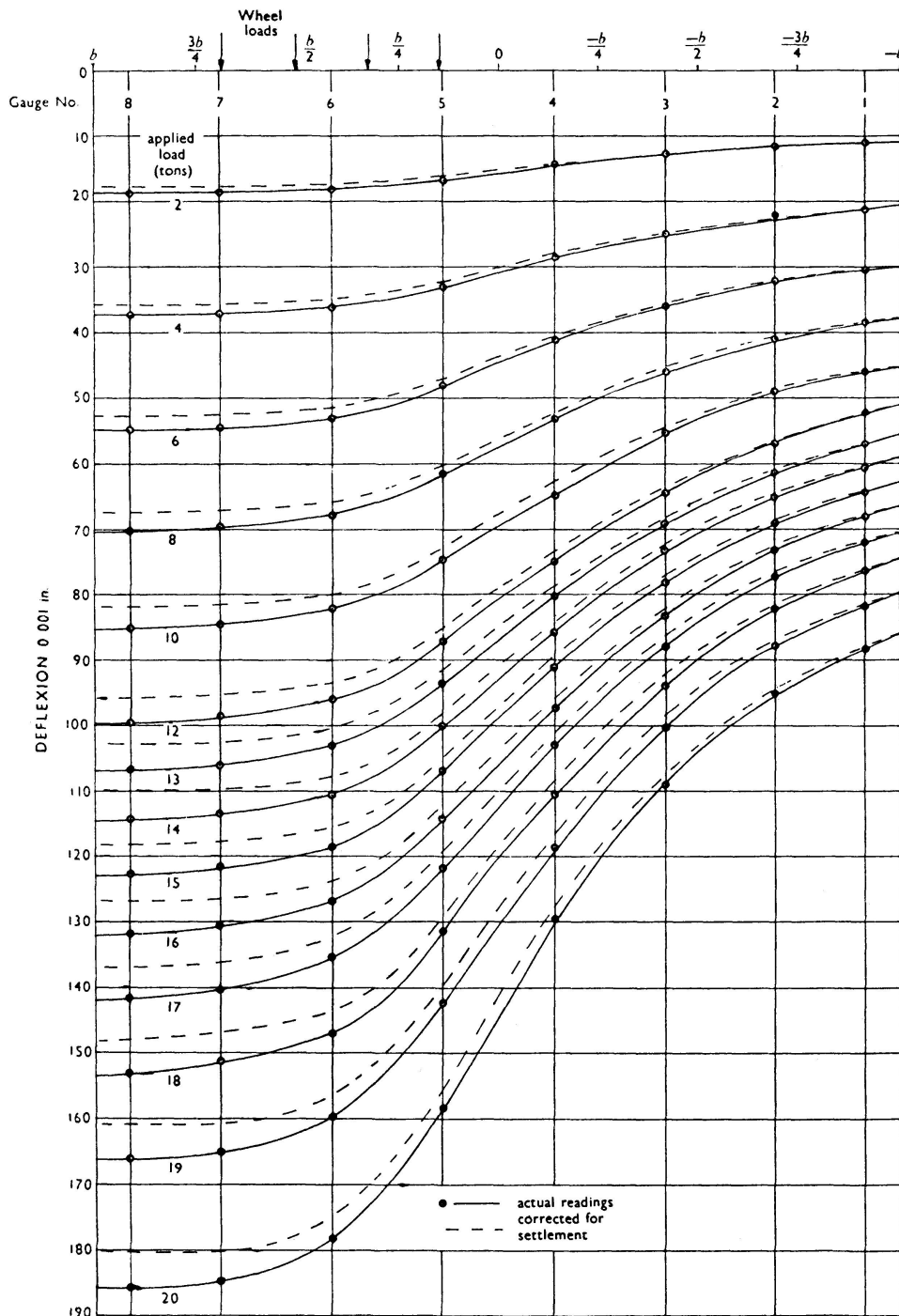
Fig. 4. Box-Section Bridge — Loading No. 6 — Transverse Deflexion Profiles.

Longitudinal Bending Moments

For a structure comprised of a number of precast units jointed together, the interpretation of strain readings is exceedingly difficult especially when shrinkage cracks are present. In order to derive distribution coefficients for moments it was assumed that the moment in each beam was proportional to the tensile strain in its bottom fibre. Profiles for the tensile strain for each stage of the various loadings were drawn and the "mean" tensile strain
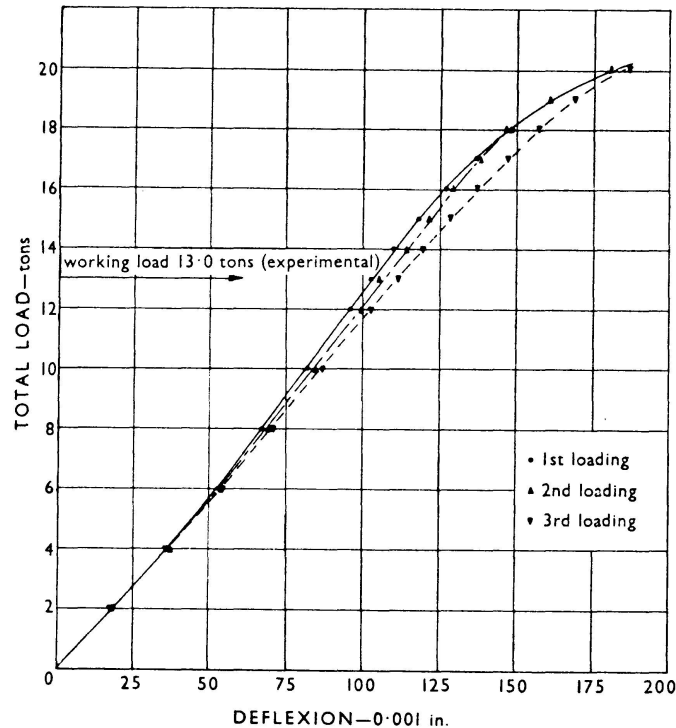
Fig. 5. Box-Section Bridge — Loading No. 6 — Load-Deflexion Curves for an Edge Beam.

deduced from these by Simpson's rule. Distribution coefficients were then obtained in a manner similar to that used for deflexions. Fig. 6 shows the theoretical and experimental distribution coefficient profiles for the various loadings. From the Figure it may be seen that for the complete 8-wheel bogie the distribution coefficients in the loaded region are in good agreement with the theoretical values provided these are increased by approximately 10 %. This applies for all the loadings with the exception of No. 4 which was outside the design range of eccentricities and corresponds to four wheels of the abnormal load bogie being on the pavement of the bridge. For this loading the necessary increase in the theoretical values was about 17 %.

Transverse Moments

With so many in situ joints in the structure, a quantitative analysis of the measured strains is virtually impossible and all that can be said is that the

transverse prestress was adequate to ensure that the theoretical distribution characteristics of the bridge were operative under design conditions.
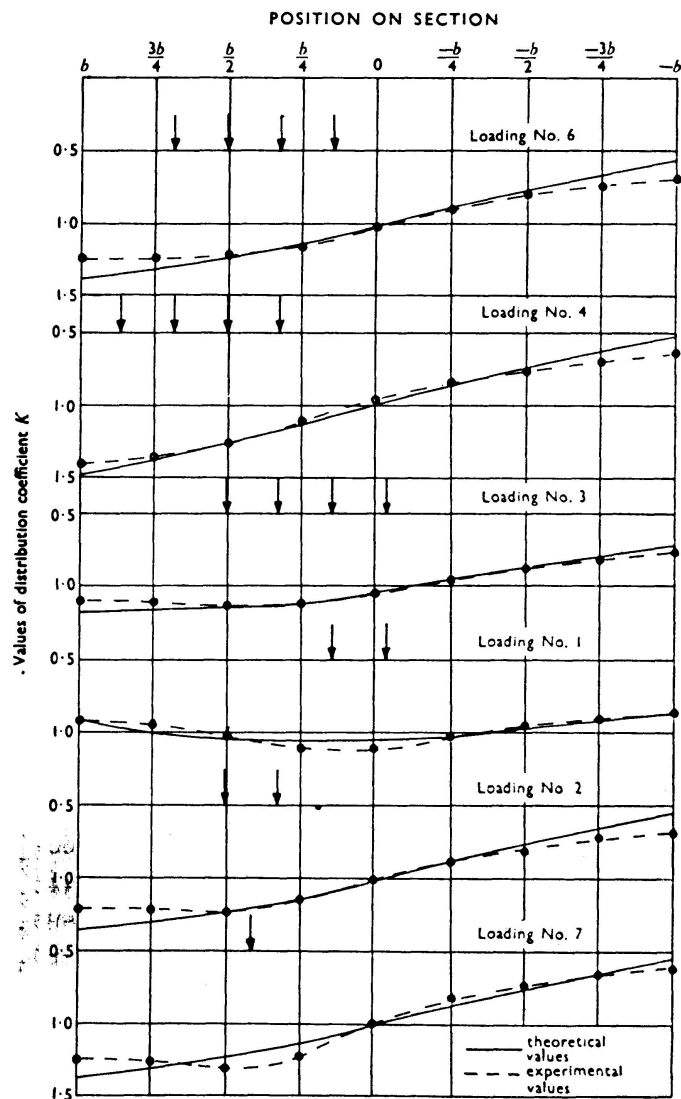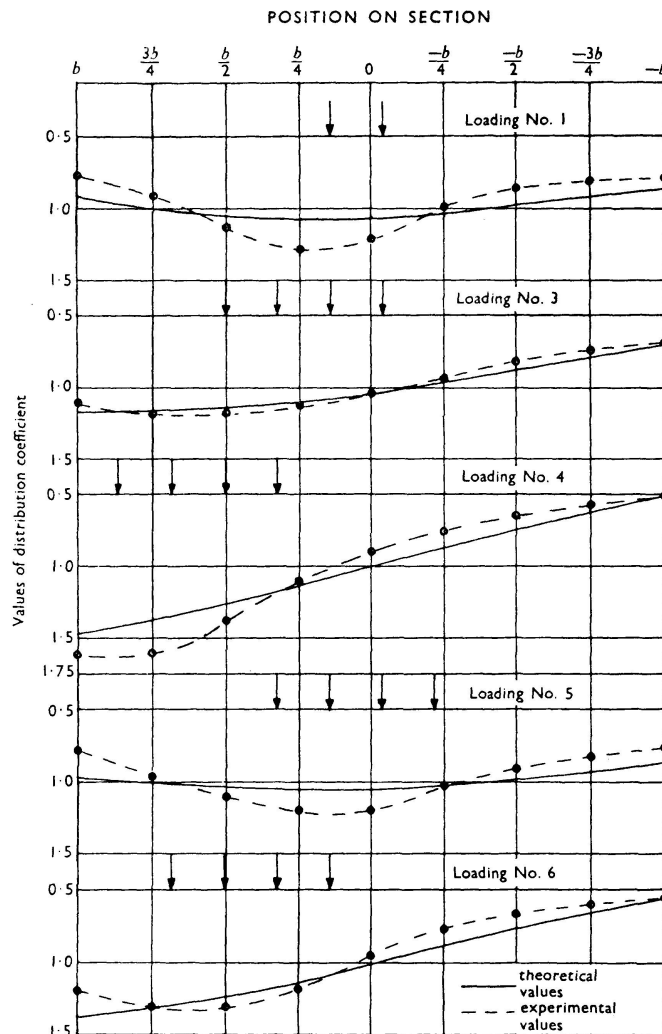

Fig. 6. Box-Section Bridge — Comparison of Theoretical and Experimental Distribution Coefficient Profiles for Longitudinal Moments for Various Loadings.

Mode of Failure

The concentrated loading No. 7 was employed in the test to failure of the bridge; for this loading both loading areas were above the web of a single beam. The first loading was applied to a maximum load of 20 tons and although transverse cracking of three beams had occurred the bridge appeared quite sound. It was evident, however, from the "mean" deflexions that the stiffness of the bridge had decreased considerably from its value in the first series of tests. The connexion between the inverted T-beams and the top slab had deteriorated once the transverse working load of the bridge had been exceeded. After the applied load had reached 20 tons it was released; the second loading commenced after a short lapse of time during which the dial gauges were

removed. On reaching a load of 18 tons it was apparent that the top slabs were not acting monolithically with the beams in the region of the load and the bridge deflected more and more at a constant load of 18 tons. When sufficient deflexion of the beam under the loads had occurred, the top slabs on either side of the transverse centre-line were virtually independent of the webs of the beams on either side of the loaded beam and with the load acting solely on the web of the beam shear failure in the web occurred. Fig. 7 shows the web of the loaded beam after two top slabs had been removed; the top

Fig. 7. Box-Section Bridge — Loading No. 7 — Shear Failure in Webs of Beams and Diaphragms.
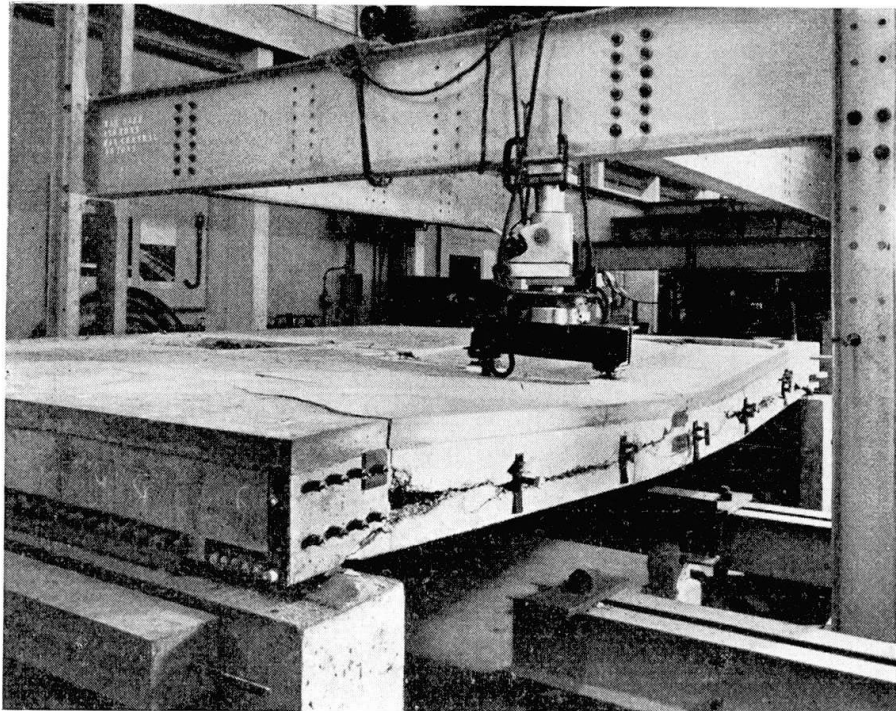
Fig. 8. Box-Section Bridge — Loading No. 8 — Torsional Failure of Edge Beams.

slabs are clearly independent of the beams and diaphragms and the high shear force in the transverse direction is indicated by the shear failure in the diaphragm in the foreground; the shear failure in the webs is clearly shown.

Thus for loading No. 7, which was a much more severe loading than that of the design bogie load, the load distribution characteristics of the bridge were perfectly satisfactory in the working load range but deteriorated rapidly for loads outside it. The failure that occurred was primarily a local failure caused by insufficient shear connexion between the beams themselves and between the beams and the top slabs.

As only about one half of the bridge was damaged by this loading, loading No. 8 was applied to ensure complete failure. A maximum load of 18 tons was applied during which torsion cracks became apparent in the upper surface of the bridge. Additional deflexion was induced at a constant load of 18 tons until the edge beam failed in torsion; this is shown in Fig. 8. The internal webs then failed in shear.

After the above analysis of the results from the tests had been carried out, it was possible to modify the design to overcome the deficiencies of the bridge. A second model bridge incorporating the modifications was therefore constructed and was tested to destruction.

Modifications in Design of Bridge

One of the main deficiencies of the bridge shown by the tests was the incompleteness of the monolithic action between the inverted T-beams and diaphragms and the top slab. The modified design therefore included a top slab cast in situ on permanent formwork, and a rearrangement of both the longitudinal and transverse prestress. Fig. 9 shows the arrangement of the prestressing wires in both the transverse and longitudinal sections. The individual beams were cast in a pre-tensioning bed and prestressed sufficiently to counteract the stress imposed by the top slab as well as the stresses due to self-weight; when the required strength was attained in the top slab, additional longitudinal wires were post-tensioned to give about the same residual stress in the bottom fibres as for the first bridge and also to give a residual compression in the top fibres thus eliminating any shrinkage cracks.

Each beam was provided with $1/4$ in. diameter mild steel stirrups, these being at 3 in. centres over the central 5 ft. of the beam and at 4 in. centres over the remainder of its length. Two $1/4$ in. diameter longitudinal bars at the top and bottom of the stirrups completed the shear reinforcing cage. The top slab was reinforced as for the first bridge except that the reinforcing mesh was continuous over the whole width of the bridge.

The transverse prestress was the same in both magnitude and position as in the first bridge but by using 0.2 in. diameter wires it was possible to get a

better distribution over the depth of the section with a number of wires passing through the bottom flanges.

Since the above modifications were made primarily to improve the ultimate strength of the bridge it was considered that a model consisting of only four

PART SIDE ELEVATION OF BEAM

TRANSVERSE SECTION OF BEAM
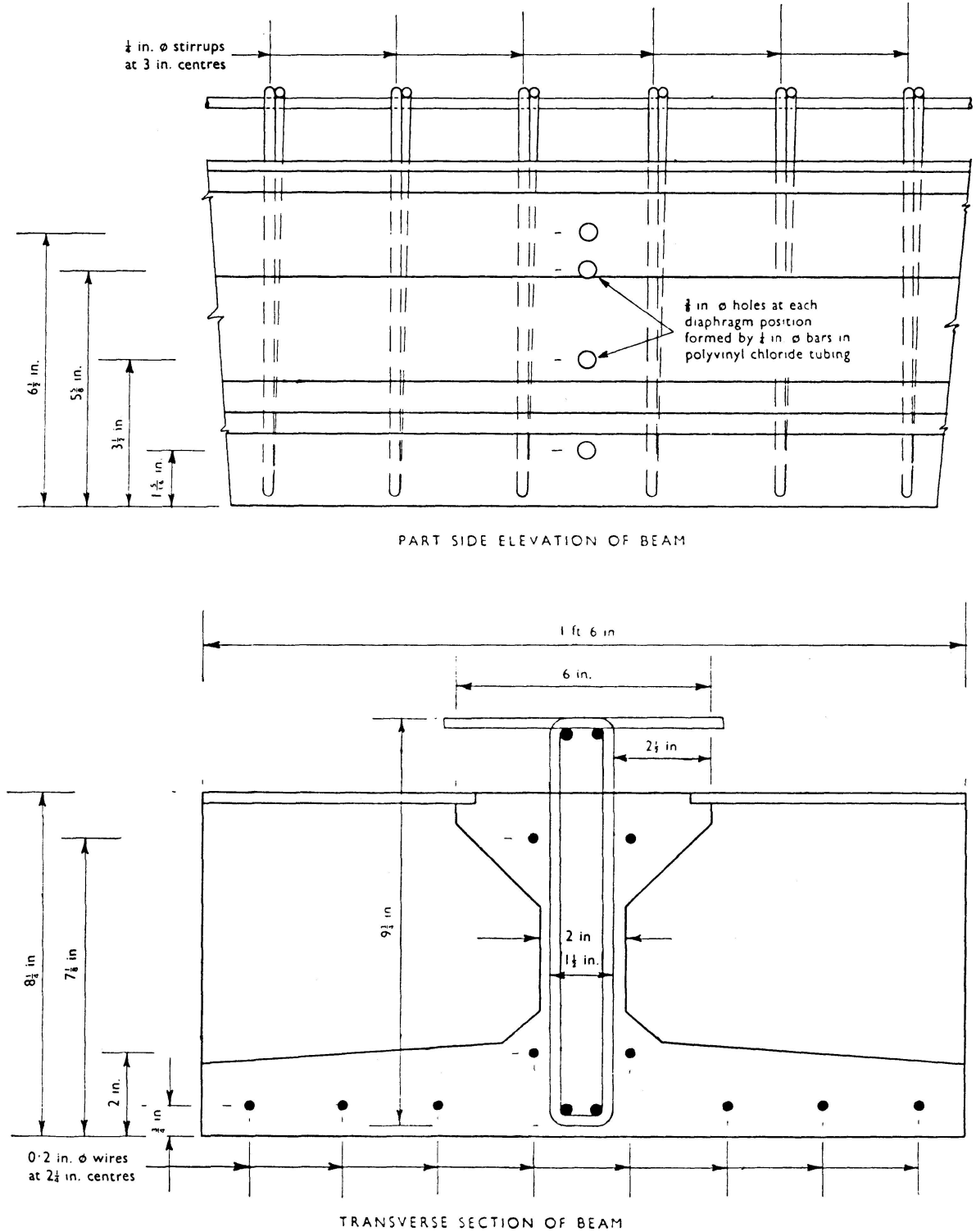
Fig. 9. Box-Section Bridge — Modified Longitudinal and Transverse Sections of Inverted T-Beam.

main beams would be adequate. With a different width it was necessary to recalculate the behaviour of the bridge in the elastic range.

Construction of Second Model Bridge

The four pre-tensioned inverted T-beams were cast on a pre-tensioning bed using a $1:1.6:1.9$ concrete by weight with a $^3/_{16}$—$^3/_8$ in. Mount Sorrel granite aggregate; the water/cement ratio was 0.45. The same mix was used for the precast diaphragms and the top slab. The average strengths obtained from 4 in. cubes were: 5,300 lb./in.^{2} at 14 days and between 8,600 and 9,600 lb./in.^{2} at the time of the tests to destruction; this variation is from the concrete of the top slab at an age of about 3 months to that of the first pre-tensioned beam at an age of 8 months.

The method of erection was exactly the same as for the first bridge except that, since there were no edge beams, it was necessary to form a number of half diaphragm units on which the transverse prestressing anchorages could bear. Panels of $^1/_4$ in. thick cement asbestos sheet were used as permanent formwork for the top slab: these panels fitted into recesses cast in both the inverted T-beams and the diaphragms. Before the top slab was cast a temporary transverse prestress was applied to prevent any movement at the joints caused by vibration. When the top slab had attained a strength of 4,500 lb./in.^{2} the four longitudinal wires were post-tensioned and then the transverse stressing carried out. All the post-tensioned wires were grouted efficiently using specially designed grouting nozzles. Fig. 10 shows the bridge before testing commenced.
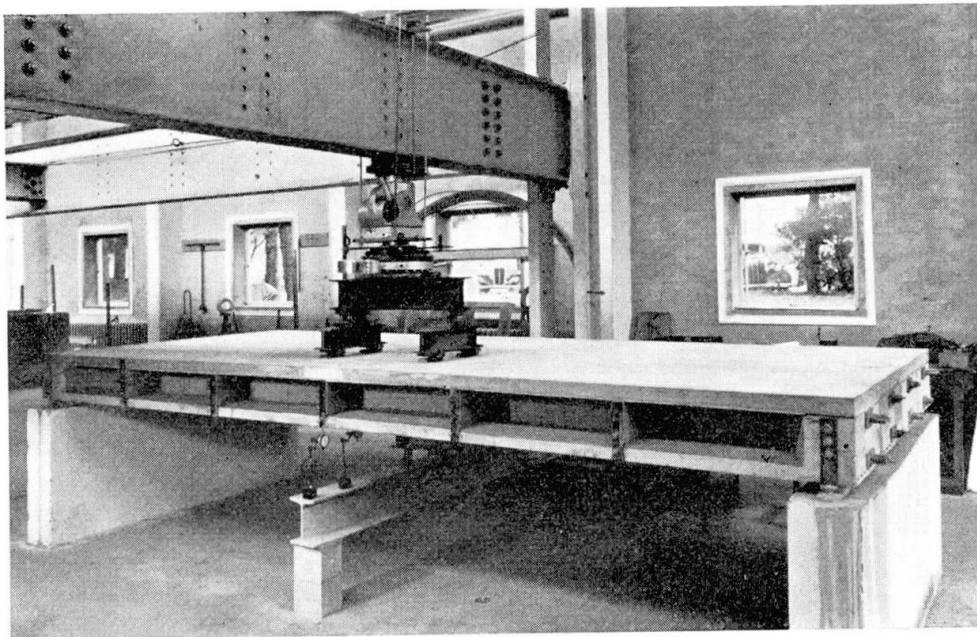
Fig. 10. Box-Section Bridge — General View of Second Bridge.

Details of Testing Apparatus and Tests Carried Out

The loading device used in testing the bridge is shown in Fig. 10. It consisted of a model of one-half of the Ministry of Transport abnormal load bogie, and thus provided a more severe loading than that used in the elastic tests on the first bridge. This loading device was placed on the bridge in such a way that the internal wheels were symmetrically placed on the web of the second beam and with respect to the transverse centre-line; the load was kept in this position throughout the tests.

Analysis and Discussion of Results

Table 2 gives the distribution coefficients and "mean" deflexions for the range of loads from 0 to 20 tons and also the corresponding theoretical coefficients. There are two points of interest in this Table: firstly, the distribution coefficients remained approximately constant well beyond the design load of 7.88 tons; even when cracking occurred the transverse strength was sufficient to maintain the distribution properties; secondly, the agreement between the theoretical and experimental values is good except at points remote from the load; the agreement is comparable with that found for the previous bridge. The actual distribution is better than the theoretical indicating that the torsional parameter was slightly underestimated.

The longitudinal strain readings in the bottom fibres were used to determine the distribution coefficients in the elastic range of the bridge. The mean values of the distribution coefficients so derived are compared with the theoretical values and those derived from the deflexion results in Fig. 11. The difference between the experimental curves for deflexion and strain has a maximum value of 7.5 % which is within the value of 10 % put forward in the load distribution analysis [1, 5].
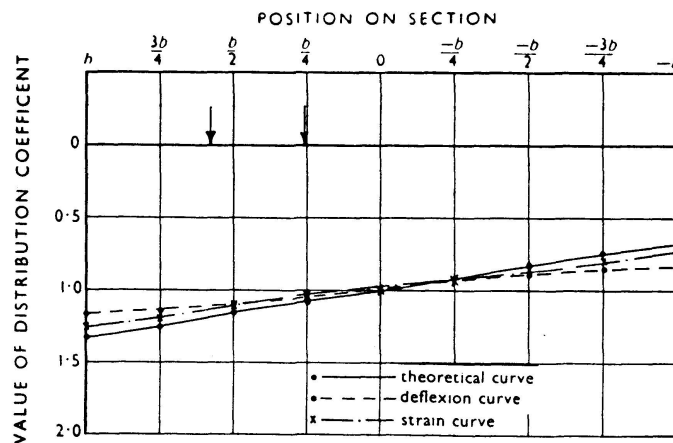
Fig. 11. Box-Section Bridge — Comparison of Distribution Coefficient Profiles for the Second Bridge.

Table 2. Box-Section Bridge — Distribution Coefficients and "Mean" Deflexions for the
Second Bridge

Load (tons)	Position on section									"Mean" deflexion (0.001 in.)
	b	$3b/4$	$b/2$	$b/4$	0	$-b/4$	$-b/2$	$-3b/4$	$-b$	
1	1.216	1.200	1.141	1.034	0.951	0.918	0.910	0.844	0.844	6.0
2	1.213	1.150	1.106	1.039	1.006	0.928	0.888	0.839	0.854	13.5
3	1.110	1.146	1.121	1.052	0.988	0.932	0.882	0.856	0.856	20.8
4	1.124	1.138	1.108	1.040	0.985	0.928	0.905	0.855	0.854	28.1
5	1.148	1.140	1.096	1.043	0.996	0.940	0.896	0.858	0.854	36.4
6	1.172	1.137	1.089	1.045	0.988	0.934	0.902	0.862	0.858	42.3
7	1.201	1.134	1.091	1.045	0.991	0.935	0.899	0.860	0.855	49.7
8	1.204	1.134	1.088	1.045	0.995	0.938	0.897	0.861	0.854	57.3
9	1.183	1.130	1.083	1.048	0.988	0.938	0.885	0.852	0.847	66.2
10	1.177	1.125	1.084	1.043	0.987	0.936	0.894	0.851	0.841	74.3
11	1.174	1.126	1.086	1.043	0.990	0.934	0.889	0.852	0.841	82.3
12	1.179	1.129	1.089	1.047	0.990	0.937	0.890	0.853	0.843	89.9
13	1.177	1.127	1.087	1.044	0.992	0.935	0.889	0.853	0.840	97.6
14	1.177	1.130	1.087	1.048	0.998	0.935	0.890	0.854	0.839	106.5
15	1.176	1.128	1.090	1.047	0.989	0.934	0.890	0.854	0.840	116.2
16	1.173	1.124	1.097	1.044	0.985	0.928	0.885	0.848	0.834	128.1
17	1.188	1.142	1.096	1.048	0.992	0.921	0.880	0.851	0.823	151.1
18	1.183	1.139	1.088	1.044	0.984	0.918	0.882	0.850	0.820	162.6
19	1.173	1.130	1.083	1.039	0.983	0.914	0.881	0.847	0.817	177.7
20	1.160	1.122	1.087	1.039	0.993	0.926	0.889	0.859	0.824	210.0
Mean value for loads from 1 to 8 tons	1.174	1.147	1.104	1.042	0.988	0.932	0.897	0.855	0.854	
Theoretical values	1.339	1.270	1.162	1.086	1.003	0.926	0.841	0.759	0.678	

Thus from elastic considerations the behaviour of this model was comparable with that of the first bridge although the modifications appear to have increased the torsional parameter slightly. Further the in situ slab and the elimination of shrinkage cracking ensured monolithic behaviour throughout the elastic range.

Cracking of the edge beam nearer the load occurred at a load of about 11 tons. The distribution of deflexion, however, remained approximately constant for loads in excess of this figure showing that redistribution of moments was taking place. Thus between 11 tons and 20 tons the cracks travelled progressively across to the remote edge beam. The cracks were all

due to longitudinal bending and crossed the transverse joints; they were fairly uniformly distributed and extended to about half the depth of the web in the edge beam nearer the load.

At this stage the deflexion gauges were removed and only the edge deflexions were subsequently measured (using a tape). The load was increased steadily until it reached 25 tons; the pattern of cracks on the soffit at this load is shown in Fig. 12. The load was increased further until at 29 tons the concrete crushed in the top flange of the edge beam. This crushing extended
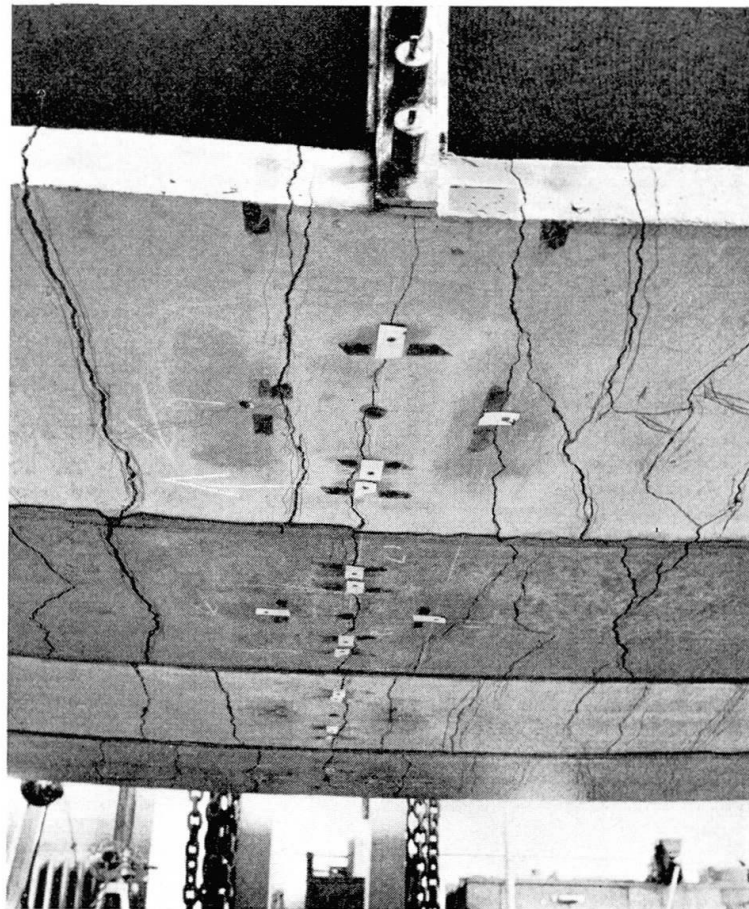
Fig. 12. Box-Section Bridge — Crack Pattern on Soffit of Second Bridge at an Applied Load of 25 Tons.

from the centre of the edge beam along two diagonal lines to the external wheels of the loading device and then transversely to the internal wheels. At failure the depth of the compressive stress block in the edge beam was about 0.75 in.; this is in reasonable agreement with the calculated 0.89 in. The maximum recorded deflexion was $3\,^{15}/_{16}$ in. at the edge nearer the load; at the remote edge the deflexion was $3\,^{1}/_{16}$ in.

Description of the Composite Slab Bridges [6—8]

Three composite slabs have been tested; the slabs consisted of precast prestressed inverted T-beams, in situ concrete of different qualities and varying amounts of transverse mild steel reinforcement. To obtain one of the limiting cases it was thought necessary to test one slab which had no transverse steel. It was not considered necessary to test a composite slab with transverse prestress determined from a load distribution analysis since previous tests [9, 10] have provided sufficient information on the behaviour of two way prestressed slabs under elastic and ultimate load conditions.

Bridge No. 1

The plan dimensions of the bridge were 10 ft. span and 11 ft. 4 in. width; these dimensions were derived on the basis that the bridge was a one-third scale model of a 30 ft. span bridge carrying a 24 ft. carriageway and two 5 ft. footpaths.

The bridge was designed for the Ministry of Transport standard loading with the increase suggested by HOLLAND [11] to cover the effect of the abnormal load. For the particular scale used for the bridge the Ministry of Transport standard loading was equivalent to 220 lb./ft². together with a knife-edge load of 900 lb./ft. width; for an equivalent 30 ft. span bridge the suggested increase is 25 % and therefore this figure was used. The design was only carried out for the longitudinal moments.

Since the test was to find the effect of abnormal loading, the working load used throughout this section of the paper implies the abnormal loading which, for one-third scale on a 30 ft. span bridge, consists of one bogie with a total load of 10 tons.

The concrete used in the beams consisted of $^3/_8$—$^3/_{16}$ in. Mount Sorrel granite, Heston sand, and ordinary Portland cement; the aggregate/cement ratio was 3.3 and the water/cement ratio 0.43. The concrete was placed using Kango hammers on the formwork and when it had taken its initial set the steel bars forming the holes for the transverse steel were removed and the top surface was brushed to expose the aggregate. The holes through the webs of the beam were of $^5/_8$ in. diameter with their centres 2 in. above the soffit; the holes were at 8 in. centres over the central 4 ft. and at 12 in. centres over the remaining sections of the beams. Since no transverse steel was incorporated in the first composite slab the holes were not necessary but for obvious reasons, a standard mould was used for the precast units in all the slabs.

The joints between the end blocks were packed with a dry mortar and the shuttering for the in situ concrete was erected. The in situ concrete was then placed; the mix used was the same as for the precast units. The depth of the composite slab was 6 in.

The stress conditions in both the precast and the composite section under the various types of loading are given in detail in Appendix 1, together with the properties of the section.

Bridge No. 2

This bridge slab was similar in every respect to bridge No. 1 apart from the slightly greater age of the precast units, the slightly lesser age of the in situ concrete and the presence of mild steel transverse reinforcement. This reinforcement consisted of $1/4$ in. diameter mild steel bars, hooked at one end, which were placed through the transverse holes so that each bar occupied the bottom portion of the hole.

A general view of the second bridge is shown in Fig. 13.
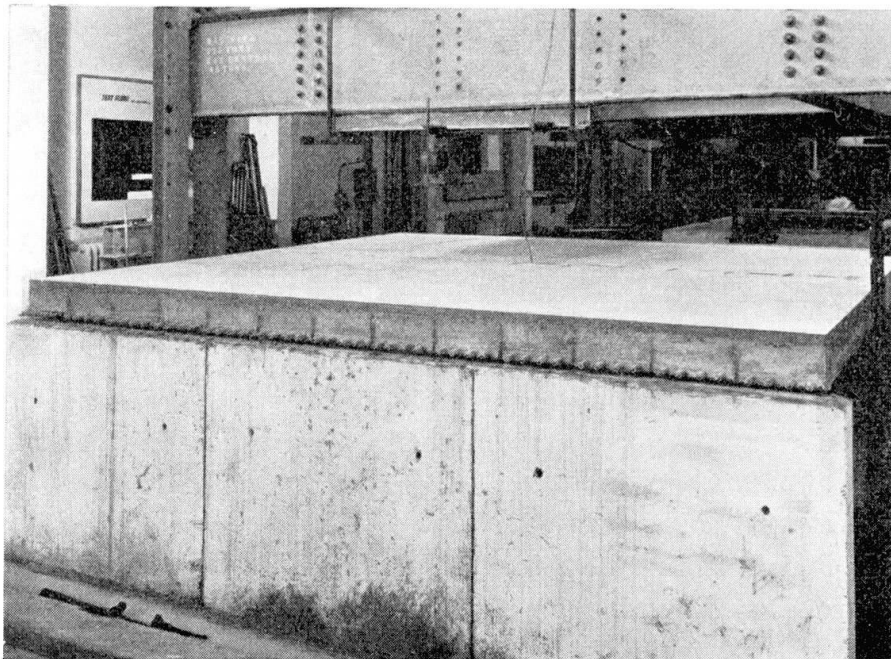
Fig. 13. Composite Slab Bridges — General View of One of the Bridges.

Bridge No. 3

This bridge slab was similar in every respect to bridge No. 2 apart from the quality of the in situ concrete. The mix used had an aggregate/cement ratio of 5.3 and a water/cement ratio of 0.6; the materials used were similar to those used throughout the series of tests.

Details of the Test Loading and Tests Carried out

The loading device was a representation to one-third scale of one bogie of the Ministry of Transport abnormal load, i.e. eight equal loads on two axles

with the loads at 1 ft. centres transversely and the axles at 2 ft. centres. Each load was applied through a $5 \times 2 \times 1/2$ in. steel pad bearing on felt.

Two positions of the loading device were used; these are shown in Fig. 14. The two positions shown in this Figure will be referred to as the central and eccentric loadings. These two positions give the maximum transverse moment condition and, approximately, the maximum longitudinal moment condition for the form of bridge slab considered.

In general, for each bridge, the central loading was first applied in stages up to a total load of 5 tons and this loading was repeated until all the deflexion
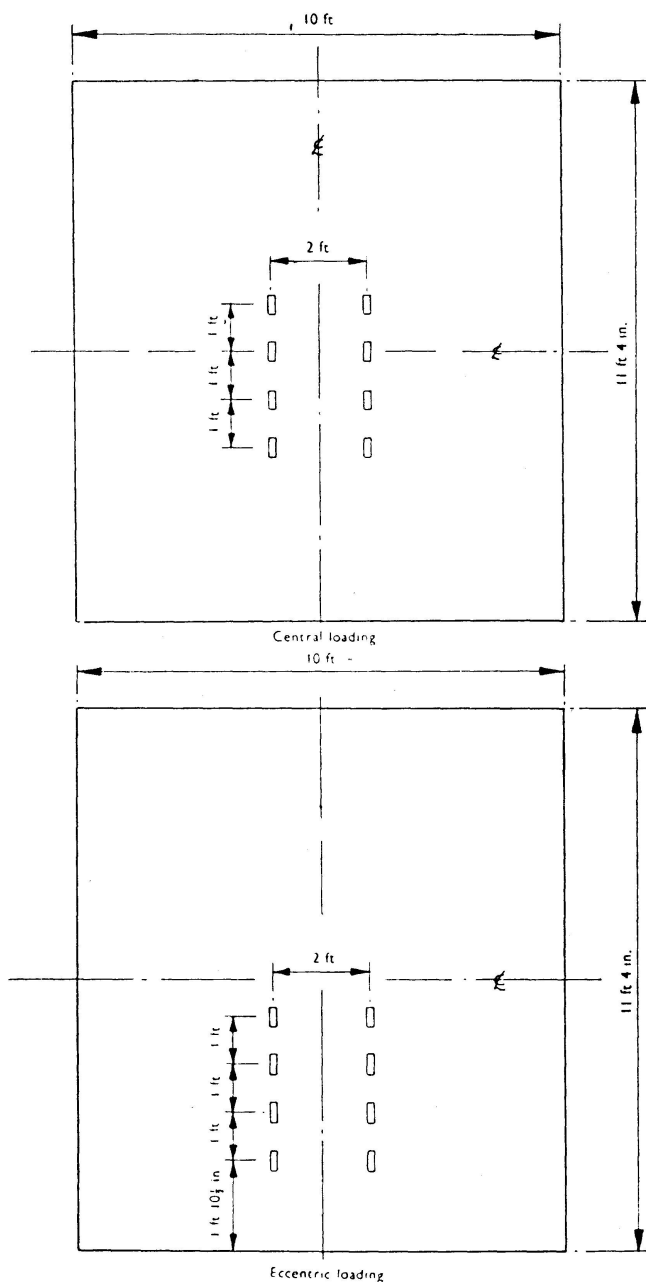
Fig. 14. Composite Slab Bridges — Positions of Loading Device.

and strain measurements had been obtained. The process was repeated for total loads up to 10 tons and then for total loads up to 15 tons. The loading device was then moved to the eccentric loading position and an identical series of tests carried out. Finally, the bridge was loaded to destruction with the loading device in the central loading position.

Analysis and Discussion of Results

Table 3 gives details of the average concrete strengths at various ages for the concrete used in the manufacture of the precast beams for each bridge.

Table 3. Composite Slab Bridges — Average Cube Strengths (lb./in.²) of Concrete Used in the Manufacture of the Precast Beams for the Three Bridges.

Age	7 days	14 days	28 days
Bridge No. 1	4850	6020	7400
Bridge No. 2	4450	5760	6850
Bridge No. 3	5070	6270	6780

Table 4 gives details of the cube strength of the in situ concrete used in the three bridges. The modulus of rupture specimens for the in situ concrete were tested at the same time as the first loading tests on each bridge; for bridge No. 1 the modulus of rupture was found to be 850 lb./in². and for bridge No. 3 600 lb./in². Unfortunately no prisms were made when the in situ concrete was cast for bridge No. 2 and hence no data are available regarding the modulus of rupture of the concrete.

Table 4. Composite Slab Bridges — Cube Strengths (lb./in.²) at Various Ages for the in Situ Concrete Used in the Three Bridges

Age	7 days	28 days	At time of test to failure
Bridge No. 1	5025	7830	10,050
Bridge No. 2	—	6900	7590
Bridge No. 3	2920	4200	4810

Reinforcing Steel

Three sample lengths of the reinforcing steel were tested to determine the yield point and Young's modulus; the yield point was 38,600 lb./in². and Young's modulus 28.6×10^6 lb./in².

Loading Tests — Deflexions

a) *Central loading.* For each stage of loading the "mean" deflexion of each bridge was calculated by applying Simpson's rule to the thirteen individual beam deflexions; these "mean" deflexions are given in Tables 5, 6 and 7. In each of these Tables the "loading number" is given; this is the total of number of times the bridge had been loaded in order to obtain all the deflexion and strain readings. As may be seen from the Tables, in each bridge the "mean" deflexion at any specific load remained sensibly constant even after overloads of up to 1.5× Working load had been applied many times. If the average "mean" deflexions (given in Tables 6, 7 and 8) are compared at various proportions of the working load then it is found that for the three bridges, considered in the order of No. 1 to No. 3 the "mean" deflexions were in the ratio of 1 : 1.11 : 1.25 at 0.5, 1.0 and 1.5 times the working load. This difference in "mean" deflexion may be taken as representing the difference in effective Young's modulus for the various composite slabs.

From the curves relating load to "mean" deflexion for the three bridges it was clear that the stiffness properties changed at loads of about 20, 15 and 12 tons respectively in the three bridges; this indicates that the cracks between the bottom flanges of the longitudinal beams were becoming sufficiently wide to change the form of the distribution for the slabs. It is also of interest to note that, for each slab, even after overloads greater than 2 × Working load, the "mean" deflexions at the working load were not changed appreciably, the change being in every case less than 10 %.

From the initial portion of these curves an estimate of the effective Young's modulus for each composite slab was obtained; the values found were 6.22×10^6 lb./in.^{2}, 5.69×10^6 lb./in.^{2} and 4.85×10^6 lb./in.^{2} for the first, second and third slabs respectively.

The distribution coefficients, K, for each bridge were derived from the actual deflexions of the individual beams and the experimental "mean" deflexions obtained at any specific stage of loading. Typical values of the distribution coefficients, obtained for various ranges of load, for the three bridges are given in Table 8; much more detailed information can be obtained from the individual reports on each bridge test [6, 7, 8]. All the values in this Table were obtained after considerable numbers of loading cycles. From the Table it may be seen that the distribution properties of each bridge remained sensibly constant up to 1.5 × Working load despite the relatively large number of loading cycles applied to each bridge; for the values quoted in the Table the bridges had sustained at least 60 cycles of loading.

For bridge No. 1 the distribution coefficients up to a load of 0.5 working load were in good agreement with those for an isotropic slab when the load was first applied; beyond that load the maximum distribution coefficients deteriorated slightly as the transverse bending moments caused cracking of

Table 5. Composite Slab Bridge No. 1 — Comparison of "Mean" Deflexions (0.0001 in.)

Total load (tons)	Loading number												Average of "mean" excluding last reading	Range (%)
	1	10	11	29	30	41	51	61	71	72	73	74		
1	49.3	49.4	—	—	—	53.5	—	—	—	—	—	—		
2	100.2	99.0	99.8	100.5	101.2	104.1	—	—	—	—	—	—		
3	149.5	148.7	—	—	—	154.2	—	—	—	—	—	—		
4	200.3	199.6	199.6	201.9	202.0	206.1	—	—	—	—	—	—		
5	252.2	250.0	—	—	—	260.7	256.7	253.5	259.0	251.0	251.8	264.3	255.5	{+2.8 / -2.0}
6			304.0	306.6	305.7	309.7	313.7	—	—	—	—	—		
7			357.3			360.5	361.1							
8			408.5	411.7	411.4	413.8	413.8							
9			464.6			466.1	468.8							
10			521.7	516.8	518.4	517.6	522.5	513.5	524.6	505.0	520.7	573.8	518.1	{+1.3 / -2.5}
11				575.3	572.5		579.7							
12				630.3	626.1		635.4							
13				688.9	679.7		692.5							
14				745.2	733.5		746.3							
15				805.3	787.9		810.9	779.6	798.1	788.0	785.0	1,018.1	793.0	{+1.8 / -1.7}
16								837.1						
17								895.9						
18								959.6		946.0	947.3			
19											1,003.6			
20											1,059.3	1,885.9		
21											1,133.8			
22											1,201.7	—		
23											1,300.3	2,553.2		
24											1,443.0			
25											1,588.0			
26											2,128.9			
Position of vehicle	C	C	C	C	C	E	E	C	E	C	C	C		

C = central, E = eccentric

Table 6. Composite Slab Bridge No. 2 — Comparison of "Mean" Deflexions (0.0001 in.)

| Total load (tons) | Loading No. | | | | | | | | | | Average of "mean" excluding last reading | Range (%) |
	1	2	51	61	77	78	102	103	104	105		
1	48.1	56.2	54.9	51.5	54.1	56.4						
2	102.7	111.1	106.6	106.5	110.6	111.2						
3	157.9	165.5	162.5	159.4	166.9	168.2						
4	214.5	222.7	218.6	216.6	224.3	223.4						
5	266.8	278.0	276.9	279.3	282.4	284.8	279.9	284.0	277.0		282.1	{−5.4 {+1.0
6	328.5	337.8	334.5	334.8	342.5	341.2						
7	385.1	392.1	391.8	395.4	403.6	400.2						
8	445.7	453.6	451.9	455.6	461.6	459.6						
9	508.0	509.9	509.1	516.7	524.7	518.9						
10	572.5	574.7	569.8	576.3	586.2	582.9	578.9	582.0	583.0		578.5	{+2.8 {−4.5
11			630.0	634.0	649.6	643.1						
12			688.3	694.0	711.9	707.4						
13			754.4	755.7	774.3	769.1						
14			819.9	825.9	838.6	829.1						
15			888.8	874.9	904.9	895.0	872.6	883.0	880.0	1,075	885.6	{+2.2 {−1.5
16								950.0	959.0			
17								1,019.0	1,019.0			
18								1,080.1	1,082.0	1,577		
19									1,142.0			
20									1,220.0			
21									1,297.0	2,403		
22									1,390.0			
23									1,513.0			
24									1,673.0	3,485		
25									1,979.0	3,781		
26									2,404.0	4,234		
Position of vehicle	C	C	C	C	E	E	C	C	C	C		

C = central, E = eccentric

Table 7. Composite Slab Bridge No. 3 — Comparison of "Mean" Deflexions (0.0001 in.)

Total load (tons)	Loading number									Average of "mean" exclud. last reading	Range (%)
	1	38	39	80	81	199	200	201	202		
1	61.6	58.8		61.2	60.4						
2	125.5	121.3	122.0	122.2	120.0			151.0			
3	190.8	184.0		187.0	181.7						
4	254.4	247.4	248.0	251.2	245.2			270.4			
5	322.9	312.8		319.7	307.3	321.8	321.0		333.0	317.6	$\left\{\begin{array}{l}+1.7\\-3.2\end{array}\right.$
6	389.4	378.1	375.4	383.0	370.2			402.0			
7	457.1	443.8		449.0	435.4						
8	526.8	506.3	504.0	515.8	499.7	530.5		524.8			
9	599.0	571.9		580.3	565.5						
10	665.9	638.6	638.2	647.5	626.7		651.9	667.5	661.0	645.8	$\left\{\begin{array}{l}+3.3\\-2.9\end{array}\right.$
11			705.1	714.7	696.7						
12			771.9	776.7	761.4			804.6			
13			842.2	850.6	832.4						
14			907.1	917.1	899.3			939.6			
15			977.8	982.8	972.1	977.8	987.6		1,100.0	979.6	$\left\{\begin{array}{l}+0.8\\-0.8\end{array}\right.$
16							1,052.1	1,083.3			
17							1,132.3	1,160.0			
18							1,211.5	1,232.6			
19								1,299.5			
20								1,382.9	1,857.0		
21								1,464.5	2,074.0		
22								1,579.3	2,240.0		
23								1,742.2	2,426.0		
24								1,922.1	2,647.0		
25								2,131.6	2,955.0		
Position of vehicle	C	C	C	C	E	C	C	C	C		

C = central, E = eccentric

Table 8. Composite Slab Bridges — Central Loading — Average Distribution Coefficients at Beam Positions for Various Ranges of Load

Bridge No.	Range of load (tons)	Beam No.												
		1	2	3	4	5	6	7	8	9	10	11	12	13
1	0—5	0.972	1.018	1.056	1.112	1.154	1.172	1.135	1.073	0.987	0.892	0.822	0.745	0.688
	5—10	0.965	0.999	1.045	1.104	1.147	1.165	1.136	1.076	0.983	0.888	0.827	0.760	0.710
	10—15	0.954	0.994	1.042	1.103	1.156	1.178	1.144	1.077	0.993	0.899	0.821	0.757	0.703
2	0—5	0.928	0.971	1.047	1.062	1.199	1.207	1.166	1.118	1.006	0.895	0.805	0.742	0.665
	5—10	0.918	0.965	1.035	1.088	1.181	1.193	1.158	1.110	1.002	0.903	0.815	0.744	0.687
	10—15	0.914	0.966	1.032	1.096	1.178	1.191	1.156	1.103	0.995	0.899	0.813	0.746	0.694
3	0—5	0.916	0.931	1.016	1.102	1.137	1.147	1.136	1.090	1.034	0.942	0.850	0.781	0.760
	5—10	0.905	0.956	1.009	1.080	1.132	1.159	1.147	1.088	1.027	0.937	0.849	0.777	0.742
	10—15	0.912	0.944	1.011	1.082	1.130	1.162	1.152	1.100	1.032	0.935	0.851	0.783	0.739
Theoretical values for an isotropic slab		0.952	0.992	1.035	1.082	1.113	1.130	1.117	1.076	1.023	0.962	0.895	0.838	0.786

Table 9. Composite Slab Bridges — Eccentric Loading — Average Distribution Coefficients at Beam Positions for Various Ranges of Load

Bridge No.	Range of load (tons)	Beam No.												
		1	2	3	4	5	6	7	8	9	10	11	12	13
1	0—5	1.673	1.555	1.471	1.382	1.244	1.135	0.997	0.861	0.734	0.628	0.517	0.447	0.358
	5—10	1.566	1.496	1.443	1.377	1.265	1.144	1.012	0.876	0.752	0.648	0.542	0.467	0.386
	10—15	1.560	1.482	1.449	1.381	1.271	1.146	1.010	0.874	0.746	0.636	0.550	0.455	0.390
2	0—5	1.369	1.409	1.415	1.334	1.324	1.199	1.023	0.910	0.768	0.647	0.567	0.496	0.459
	5—10	1.375	1.399	1.405	1.346	1.304	1.181	1.025	0.904	0.763	0.653	0.569	0.508	0.481
	10—15	1.384	1.392	1.401	1.363	1.305	1.181	1.030	0.898	0.759	0.653	0.568	0.514	0.479
3	0—5	1.364	1.354	1.374	1.321	1.228	1.147	1.040	0.915	0.812	0.709	0.620	0.553	0.503
	5—10	1.374	1.360	1.350	1.307	1.238	1.161	1.040	0.909	0.816	0.699	0.626	0.561	0.513
	10—15	1.374	1.366	1.356	1.320	1.245	1.157	1.040	0.906	0.808	0.695	0.617	0.554	0.505
Theoretical values for an isotropic slab		1.300	1.294	1.282	1.257	1.206	1.134	1.043	0.948	0.854	0.770	0.696	0.633	0.580

the in situ concrete between the bottom flanges of the precast beams. As can be seen from Table 8 the deterioration was about 4 % on the values for an isotropic slab at 1.5 × Working load and it increased to a maximum of 16 % at 2 × Working load.

For bridge No. 2 the maximum distribution coefficients were about 7 % worse than those for an isotropic slab (see Table 8) for loads up to 1.5 × Working load, and there was no significant increase in the coefficients at 2 × Working load.

For bridge No. 3 the maximum distribution coefficients were about 3 % worse than those for an isotropic slab for loads up to 1.5 × Working load, and, as for bridge No. 2, there was no significant increase in the coefficients at 2 × Working load.

After the application of the first series of loads, which produced cracking between the flanges of the precast beams, the recovery of each bridge was very good. This recovery was taken as being the residual deflexion, after removal of the load, expressed as a percentage of the maximum deflexion recorded under load. For loads up to 1.5 × Working load the recovery of the bridges was about 4 % for bridge No. 1, about 5 % for bridge No. 2 and about 3 % in bridge No. 3.

b) *Eccentric loading.* The "mean" deflexions for this loading are included in Tables 5, 6 and 7. As may be seen from the Tables there was no significant difference between the "mean" deflexions for the central and eccentric loading.

The typical average distribution coefficients for various ranges of loading are given in Table 9; the values near the loaded edge for the range of load 0—5 tons for bridge No. 1 were slightly greater than those for subsequent load ranges because account could not be taken of the abutment settlements which, in subsequent load ranges were virtually constant. With deflexion gauges on every other beam it was not possible to assess the abutment deflexion profile accurately; in the other bridge tests dial gauges were provided on every beam and this inaccuracy was avoided.

If the experimental distribution coefficients are compared with the theoretical values, also given in Table 9, the maximum coefficients are found to differ by about 20, 9 and 6 % for the bridges considered in sequence. However, the position in the width of the slab at which the maximum coefficient occurred differed in bridge No. 2 from that in the other bridges, being at beam No. 3 instead of beam No. 1. It is also of interest to note from Table 9 that the behaviour of each bridge from the distribution point of view was essentially stable for ranges of load up to 1.5 × Working load.

The recovery of the bridges for this loading was again good for loads up to 1.5 × Working load, the residual deflexion was about 4 % of the maximum deflexion under load for bridge No. 1, and about 5 % for bridge Nos. 2 and 3.

Loading Tests — Strains

a) *Central loading.* From the "mean" strains for bridge No. 1 the value of Young's modulus was determined for the two concretes on the assumption that the bridge acted effectively as a slab for loads up to 1.5 × Working load; the values were found to be 6.06×10^6 and 6.40×10^6 lb./in.^{2} for the in situ and precast concrete respectively. The average value 6.23×10^6 lb./in.^{2} agrees with the value found from the "mean" deflexions. Similarly for bridge No. 2, the values were found to be 5.62×10^6 and 6.04×10^6 lb./in. with an average value of 5.83×10^6 lb./in.^{2} which is in reasonable agreement with the value found from the "mean" deflexions.

The "mean" strains on the top and bottom fibres for bridge No. 3 differed by an amount which was less than that found for bridges Nos. 1 and 2; the bottom fibre strains were greater than those found for the other bridges, which was anticipated from the greater deflexions, but the top fibre strains were not significantly greater than those found for bridge No. 2. From the lower cube strength of the in situ concrete compared with that in bridge No. 2 it was expected that the top fibre strains would be about 1.1 times the bottom fibre strains. It seems likely therefore, that in this bridge T-beam behaviour predominated, this is supported by the discrepancy between the Young's Modulus values of 5.37×10^6 lb./in.^{2}, found assuming slab action, and the value of 4.85×10^6 obtained from the "mean" deflexions.

From the actual strains at the beam positions and the "mean" strains, distribution coefficients for the strains in both the top and bottom fibres were derived. There was not any significant difference between the two sets of coefficients for any particular load stage and therefore only the average coefficients are given in Table 10. As the Table shows there was some scatter in the results for the coefficients particularly in the region of the applied loads, caused probably by the local effects. In general, however, the distribution coefficients for each bridge were sensibly constant for loads up to 1.5 × Working load. If the maximum distribution coefficients obtained for each bridge are compared with the corresponding theoretical value the discrepancies are found to be 5, 7 and 7 % for bridges No. 1, 2 and 3 respectively.

From the maximum measured strains and the derived values of Young's modulus, the maximum stresses in the bottom fibre of the precast beams were derived; these stresses are compared with the theoretical stresses for an isotropic slab in Table 11. It should be noted that the theoretical values include the increase of 10 % which is associated with the load distribution analysis. If the distribution coefficients for deflexions and strains are compared (Tables 8 and 10) it may be seen that for these composite slab bridges the difference between the two sets of coefficients was less than 10 %. Thus, the combined effect of a poorer distribution than an isotropic slab and a difference between the distribution for deflexions and strains less than allowed for in the load

Table 10. *Composite Slab Bridges — Central Loading — Average Distribution Coefficients for Strain at the Beam Positions for Various Ranges of Load*

Bridge No.	Range of load (tons)	Beam No.												
		1	2	3	4	5	6	7	8	9	10	11	12	13
1	0—10	0.938	1.072	0.999	1.109	1.086	1.114	1.170	1.037	0.983	0.962	0.843	0.751	0.678
	10—18	0.995	1.141	1.026	1.038	1.116	1.159	1.087	1.038	0.991	0.951	0.797	0.749	0.680
2	0—10	0.902	0.947	1.052	1.078	1.139	1.196	1.144	1.101	1.053	0.901	0.817	0.758	0.750
	10—15	0.911	0.961	1.059	1.103	1.153	1.110	1.181	1.111	1.059	0.911	0.824	0.756	0.756
3	0—10	0.915	0.931	1.034	1.033	1.140	1.130	1.112	1.126	1.042	0.969	0.876	0.784	0.748
	10—15	0.902	0.909	1.015	1.028	1.144	1.147	1.134	1.137	1.054	0.955	0.890	0.788	0.760
Theoretical values for an isotropic slab		0.952	0.992	1.035	1.082	1.113	1.130	1.117	1.076	1.023	0.962	0.895	0.838	0.786

Table 13. *Composite Slab Bridges — Eccentric Loading — Average Distribution Coefficients for Strains at the Beam Positions for Various Loadings*

Bridge No.	Range of load (tons)	Beam No.												
		1	2	3	4	5	6	7	8	9	10	11	12	13
1	0—10	1.377	1.590	1.084	1.374	1.320	1.217	1.019	0.843	0.749	0.705	0.570	0.478	0.453
	10—18	1.385	1.566	1.124	1.368	1.315	1.192	1.026	0.831	0.769	0.693	0.574	0.493	0.444
2	0—10	1.464	1.410	1.461	1.280	1.368	1.166	1.069	1.919	0.793	0.737	0.593	0.503	0.504
	10—15	1.467	1.482	1.491	1.313	1.405	1.084	1.065	0.920	0.806	0.658	0.586	0.524	0.516
3	0—10	1.411	1.346	1.439	1.287	1.284	1.089	1.013	1.010	0.807	0.697	0.637	0.549	0.520
	10—15	1.414	1.357	1.379	1.287	1.269	1.076	0.995	1.028	0.783	0.685	0.625	0.540	0.520
Theoretical values for an isotropic slab		1.300	1.294	1.282	1.257	1.206	1.134	1.043	0.948	0.854	0.770	0.696	0.633	0.580

Table 11. Composite Slab Bridges — Maximum Stresses Recorded in Bridges

Bridge No.	Central Loading		Eccentric Loading	
	Applied load (tons)			
	10	15	10	15
1	745	1,128	1,172	1,810
2	845	1,243	1,030	1,590
3	837	1,256	920	1,400
Theoretical values for an isotropic slab	818	1,228	942	1,414

Table 12. Composite Slab Bridge No. 2 — Central Loading — Stresses in Transverse Reinforcing Steel

Stress (lb./in.^{2}) derived from strain measurement on gauge

Tot. load tons	A_1	A_2	A_3	B_1	B_2	B_3	C_1	C_3
2	228	80	215	255	94	134	188	201
4	575	108	538	645	201	403	430	349
6	820	121	780	1010	242	725	658	885
8	1074	121	1060	1410	322	888	1035	1115
10	1315	121	1290	1855	403	1140	1460	1585
12	1610	94	—	2430	483	1316	1830	1890
14	1920	108	1880	2740	644	1475	2160	2070
15	2080	94	2070	3130	685	1475	2320	2120

Gauges A and C on bar 8 in. from transverse centre-line

Gauges B on central bar

Suffix 1 refers to gauge on bar across joint between beams 6 and 7

3 refers to gauge on bar across joint between beams 7 and 8

2 refers to gauge on bar within web of precast beam No. 7

distribution analysis, was that the experimental stresses were in good agreement with those expected in an isotropic slab for loads up to 1.5 × Working load.

The form of the curves for the distribution of the transverse strains was consistent with the theoretical distribution of transverse bending moments in an isotropic slab bridge and the difference in magnitude between the top fibre strain and bottom fibre effective strain was a measure of the depth of the cracks between the precast units. At the joint between beam Nos. 6 and 7 the maximum strain occurred; this is consistent with the position of the maximum transverse moment. At this point the average ratio of the strains of the bottom and top fibres was about 1.66, 1.45 and 1.55 for the three bridges.

For bridge No. 1, the depth of the cracks between the precast units was assessed from all the test results and was found to be a maximum of 1.68 in. between beams Nos. 6 and 7 and to average 1.43 in. over the central portion of the bridge. For the remaining bridges, since the strain in the transverse reinforcing steel was measured, it was possible to draw the distribution of strain across the section between beam Nos. 6 and 7; these distributions are shown in Figures 15 and 16.

Fig. 15, which applies to bridge No. 2, shows that for loads up to 1.5 × Working load the behaviour of the bridge was stable; the relationship between the strain in the top fibre and the strain in the steel is constant despite the variations in the strain in the bottom fibre, with the neutral axis at a constant depth from the top fibre. The same stable behaviour was also found in bridge No. 3 as Fig. 16 shows. From a consideration of the equilibrium of horizontal forces for bridge No. 2, at a load of 15 tons the force/bar, for the strain given in Fig. 15, was 146 lb. whereas the compressive force in an 8 in. length of the bridge, corresponding to the spacing of the bars, was 4,270 lb. Obviously, therefore, the steel was not contributing significantly to the resistance moment of the section at this stage. Hence the effective depth of the transverse connecting medium or diaphragm was about 3.8 in., or twice the distance from the top fibre to the neutral axis. Similarly, the effective depth of the diaphragm for bridge No. 3 was about 4.4 in. This depth was obtained in the series of tests up to a maximum load of 10 tons, i. e. to the Working load; in subsequent tests to higher loads the strain gauges on the wires were not functioning so no more exact estimate of the depth of cracks was possible than that obtained from the top and bottom fibre strains.

The variation in the stress in the reinforcing steel for one typical test for bridge No. 2 is given in Table 12; the presence of the cracks between the precast units is evident from the variation in stress along any given bar. However it does not imply that the cracks had reached the level of the steel itself, but rather that the cracks produced a variation in the position of the neutral axis with a consequent variation in the stress in the steel.

b) *Eccentric loading*. In general, the "mean" strains for this loading were not significantly greater than those for the central loading at least within the working load range but, for loads greater than the working load, there was a very slight increase attributable to the additional cracking between the precast units produced by this loading.

The average distribution coefficients are given in Table 13; as will be seen there was more scatter in the results for this loading than for the central loading due to the more pronounced effect of the cracking between the precast units when the load was near the edge of the bridge and the susceptibility of strain measurement to small experimental errors.

For bridge No. 1, the maximum discrepancy between the theoretical values for an isotropic slab and the values given in Table 13 was 22 %; if the values
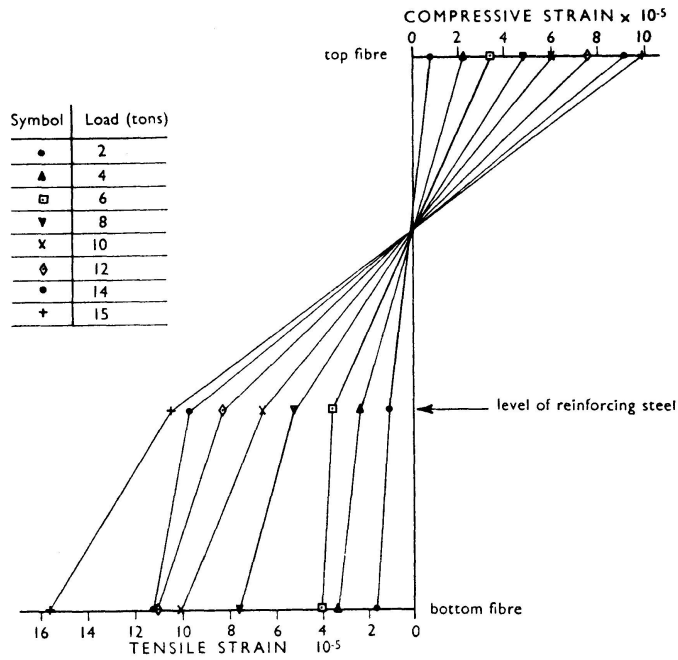
Fig. 15. Composite Slab Bridges — Bridge No. 2; Strain Distribution Across Section Between Beam Nos. 6 and 7.
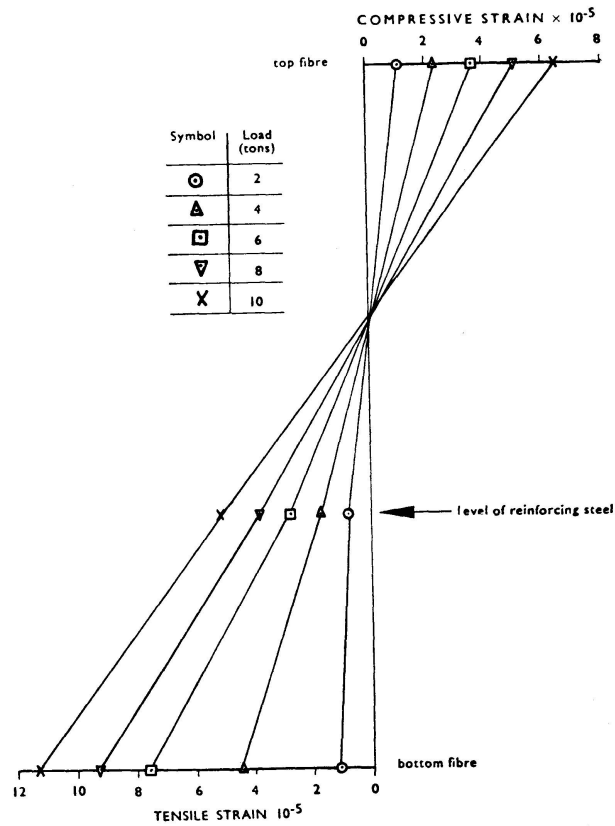
Fig. 16. Composite Slab Bridges — Bridge No. 3; Strain Distribution Across Section Between Beam Nos. 6 and 7.

given in the Table are plotted however, then the coefficient for beam No. 1 appears to be in error and the discrepancy for the estimated distribution coefficient at the edge of the bridge was about 27 %. When the distribution coefficients for both deflexion and strain are considered (Table 9 and 13), the maximum discrepancy is found to be about 5 %.

For bridge No. 2 the maximum discrepancy from the theoretical values for an isotropic slab was about 15 % and from the values obtained from the measured deflexions was about 6 %. Similarly for bridge No. 3 the two discrepancies were 11 % and 5 %.

The maximum measured stresses in the bottom fibres of the precast beams are given in Table 11; these stresses show quite clearly the difference in the distribution properties of the three bridges. The lower stresses found in the third bridge compared with the second arise from the apparent lower value of Young's modulus. The maximum measured strains did not differ by more than 2 % in these two bridges and, since the precast units in the two bridges had virtually the same concrete strengths and the distribution properties of the bridges were not very different, it seems unlikely that the maximum stresses could differ by about 14 %.

The distribution of transverse strains was of the same form as that derived on a theoretical basis for an isotropic slab. The ratio of the maximum transverse strain for the central loading to that for the eccentric loading was 1.5, 1.26 and 1.27 for bridges No. 1, 2 and 3 respectively. These ratios are again indicative of the distribution properties of each bridge and also of similarity between bridges No. 2 and 3. The stresses in the transverse reinforcing steel were of the same order as those found for the central loading; these very low stresses in the transverse steel imply that for loads up to 1.5 × Working load the steel was not contributing significantly to the behaviour of the bridge.

Loading Test — Failure

Bridge No. 1

Transverse cracking of the precast beams occurred at a load between 23 and 24 tons. For this range of loads, the maximum distribution coefficient for deflexion was 1.204. If there is an increase of 10 % in the distribution coefficient for the moments and stresses under the load, the stress in the bottom fibre should be about 2,100 lb./in.^{2}, i. e. there should be a tensile stress in the concrete of about 1,050 lb./in.^{2}. Such a stress is consistent with the modulus of rupture found from the test specimens. After the cracking mentioned above, the crack patterns developed until failure occurred at a total load of 27 tons.

Bridge No. 2

The first visible crack occurred at a load of 22 tons; this crack was along the longitudinal centre-line of beam No. 6. This crack, due to transverse
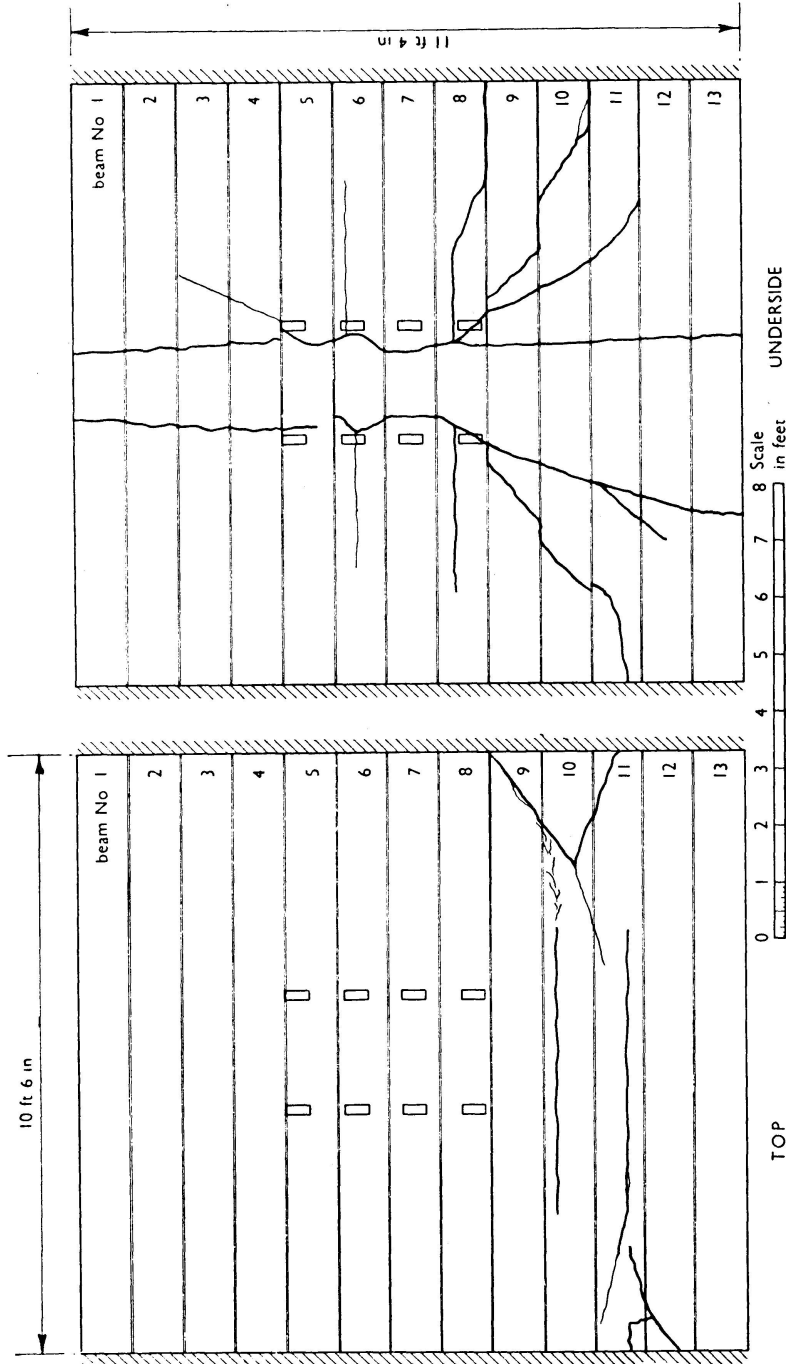
Fig. 17. Composite Slab Bridges — Bridge No. 2 — Crack Patterns on Upper and Lower Surfaces of Bridge at Failure.

bending, did not open further under subsequent loads. Transverse cracking of the beams was first noted at a load of 23 tons. At this load the maximum distribution coefficient was 1.233 and occurred at beam No. 6; assuming a 10 % increase in the distribution coefficients for the moments and stresses under the load, the bottom fibre stress should then be about 2060 lb./in.^{2} or a tensile stress in the concrete of about 1020 lb./in.^{2}. This is consistent with the modulus of rupture for beam No. 6. This transverse cracking progressed as the load was increased and extended over the entire width of the bridge at a load of 24 tons. At 25 tons diagonal cracks appeared, starting from approximately the centre of the bridge, and these increased in width with increasing load. The transverse cracks within the region covered by the diagonal cracks did not increase in width. The crack patterns shown in Fig. 17 developed until failure occurred at a load of 20 tons.

The transverse mild steel reinforcement was designed on an ultimate strength analysis as was mentioned in the introduction. It is of interest to see how this analysis relates to the failing load and mode of failure of the slab; therefore it will be given in some detail.

It was assumed that it would be uneconomic to provide sufficient transverse reinforcement to give a general transverse bending yield line across the entire width of the bridge. Therefore the yield line pattern of the type shown in Fig. 18 was assumed to occur under the central loading; the distance γ will obviously depend on the ratio of M_1 to M_2, the longitudinal and transverse sagging ultimate moments/ft. respectively. It was further assumed that the proportions of the bridge precluded the formation of a hogging yield line; this was based on the mode of failure of bridge No. 1. For simplicity the effect
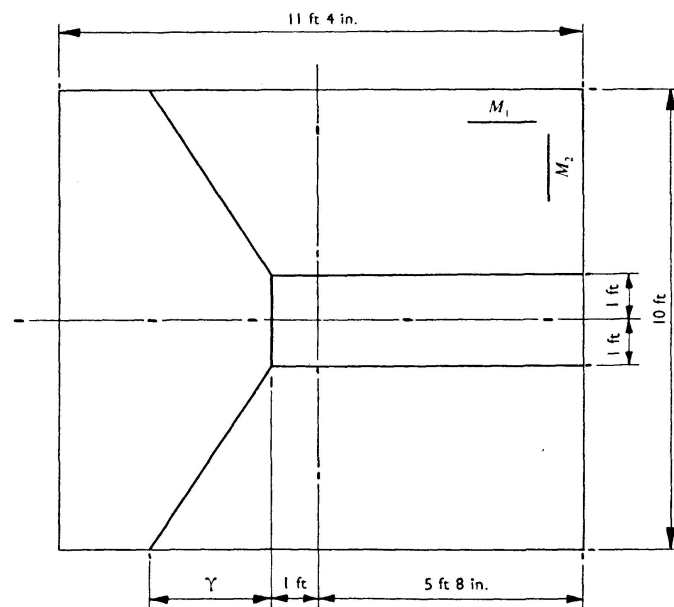

Fig. 18. Composite Slab Bridges — Assumed Pattern of Yield Lines at Failure.

of dead load was taken to be the same as if general transverse bending had occurred; this leads to an underestimation of the ultimate load.

The work equation for the system of yield lines can be written:

$$P \times 2240 + 2 \times 11.33 \times 4\,w \times \tfrac{1}{2} + 11.33 \times 2\,w$$
$$= 2\,M_1 \frac{6.67}{4 \times 12} + \frac{2\,M_1}{4 \times 12} + \frac{10\,M_2}{\gamma \times 12}, \tag{1}$$

where P = Total load at failure in tons

w = Self weight of slab in lb./ft.^{2}

γ = Unknown dimension in feet

This equation may be differentiated to obtain the minimum value of P; thus for a minimum

$$0 = \frac{2\,M_1}{48} - \frac{10\,M_2}{12\,\gamma^2}.$$

Therefore

$$\gamma = \sqrt{20 \frac{M_2}{M_1}}.$$

The values for M_1 and M_2 are derived in Appendix 2; M_1 was found to be 167,000 lb. in. and M_2, 13,650 lb. in. Thus for the minimum value of P, $\gamma = 1.28$ ft.

The substitution of this value of γ in Eq. (1), and also the value $w = 75$ lb./ft.^{2}, gives the ultimate load P. Thus

$$P = \left(2 \times 167{,}000 \times \frac{6.67}{48} + 2 \times 167{,}000 \times \frac{1.28}{48} + 10 \times \frac{13{,}650}{12 \times 1.28} - 68 \times 75\right) \frac{1}{2240}$$

$$= (4.64 \times 10^4 + 0.891 \times 10^4 + 0.888 \times 10^4 - 0.51 \times 10^4) \frac{1}{2240}.$$

Therefore $P = 26.4$ tons.

In the actual bridge the tensile strength of the concrete will provide some resistance to the formation of hogging yield lines and hence the ultimate load will be greater on this account as well as that due to the overestimation of the dead load effects.

Figure 17 shows the hogging yield lines which formed and also that the value of γ in the bridge was about 4.67 ft.

Bridge No. 3

The first visible crack occurred at a load of 23 tons; this was a transverse crack in beam No. 5. The maximum distribution coefficient at this load was 1.199; assuming a 10 % increase in the distribution coefficients for moments and stresses at this load, the bottom fibre stress should be about 2010 lb./in.^{2}, or a tensile stress in the concrete of about 970 lb./in.^{2}. This tensile stress was in reasonable agreement with the modulus of rupture for beam No. 5. Following

this initial cracking a similar crack pattern to that shown in Figure 17 developed until failure occurred at a load of 27 tons.

Using the same method of yield line analysis given in detail for bridge No. 2 the ultimate load of this bridge may be calculated. The longitudinal and transverse sagging ultimate moment per foot are derived in Appendix 2; the values were $M_1 = 195,600$ lb. in. and $M_2 = 13,580$ lb. in. Using these moments in the idealised yield line pattern shown in Figure 18, the minimum value of the ultimate load was found to be 25.3 tons with a corresponding value for γ of 1.306 ft. This theoretical ultimate load is known to be an underestimate since the dead load effects were overestimated and the tensile strength of the concrete was ignored; nevertheless the theoretical value was 0.94 of the actual failing load which is sufficiently accurate for most design purposes.

Conclusions

Box-Section Bridge

The tests have shown that this type of bridge is suitable for short spans subjected to abnormal loading, can be constructed using precast prestressed units and that a load distribution analysis accurately predicts both deflexions and stresses. The high torsional parameter of a cellular box-section structure ensures the optimum distribution characteristics without recourse to a solid slab. In the analysis, relaxation techniques were used to assess the torsional parameter; this procedure was fully vindicated by the results.

One of the difficulties emphasised by the tests was that of obtaining mono-lithic action between the various precast units. This may be overcome by casting the top slab in situ on permanent shuttering as was done in the second bridge model. However, the relatively small scale of the test structure and consequently of the joints between members was primarily responsible for this difficulty; in practice therefore it should be possible to employ either method of construction provided the detailing of the bridge is good.

At ultimate load it is possible to obtain load factors of about 2.5 on the Ministry of Transport abnormal load with this type of bridge provided mono-lithic action can be assured.

Composite Slab Bridges

This series of tests has shown that composite slab bridges can possess distribution properties under abnormal loading which are very similar to those of isotropic slabs provided that the design of the longitudinal section is based on the modified Ministry of Transport standard loading [11] and that trans-verse mild steel is provided to give a satisfactory load factor at the ultimate load; this steel should be derived from a yield line analysis.

The maximum discrepancy between the distribution coefficients found from the tests and those for an isotropic slab was 9 % if bridge No. 1, with no transverse steel is not considered; this percentage discrepancy was the same for both deflexions and moments and was that obtained after many overloadings up to a maximum of 1.5 × Working load which was taken as being the scaled down version of the Ministry of Transport abnormal load. Thus, despite the known but not visible, cracks between the flanges of the precast units the behaviour of each bridge was stable within the range of loads quoted above and furthermore the immediate recovery was very good, within 5 % of the maximum recorded deflexion under load. This recovery would obviously be even better in actual bridges due to the time interval between abnormal loadings.

At ultimate load the agreement between the actual failing load and that predicted by a yield analysis was excellent; the theoretical value under-estimating the actual value by less than 10 %. The method of calculating the theoretical ultimate load suggested in this paper is known to give a slight underestimate since the dead load effects were overestimated. For the two composite slabs containing transverse mild steel the ultimate moments transversely were 8.2 % and 8.5 % of the corresponding ultimate moments longitudinally. These figures may be compared with a value of about 41 % if a bridge of the same proportions were designed on a purely elastic method. The load factors obtained on these two bridges were 2.9 and 2.7 respectively on the abnormal loading with a factor of unity on the dead load; these factors were for the central loading and they would be reduced to about 2.0—2.1 for the eccentric loading. Such load factors are satisfactory for a structure of this type.

Appendix I

Precast Section

The properties of the precast inverted T-section were:

area	= 23.5	in.^{2}
centre of gravity from top fibre	= 3.43	in.
from bottom fibre	= 1.82	in.
second moment of area about centroid	= 61.71	in.^{4}
section modulus top fibre	= 18.0	in.^{3}
bottom fibre	= 33.9	in.^{3}
self-weight	= 24.5	lb./ft.
self-weight stresses at mid-span on a 10 ft. span		
top fibre	= 204	lb./in.^{2}
bottom fibre	=−108	lb./in.^{2}

stresses due to dead weight of in situ concrete

top fibre	$= 343$ lb./in.^{2}
bottom fibre	$= -181$ lb./in.^{2}

Composite Section

The design loading for the longitudinal moments was taken as the Ministry of Transport standard loading, to the appropriate scale, increased by 25 %. The maximum longitudinal moment per foot width was therefore

$$1.25 \left(\frac{220 \times 10^2}{8} + \frac{900 \times 10}{4} \right)$$

$$= 1.25 \ (2{,}750 + 2{,}250)$$

$$= 6{,}250 \ \text{lb. ft.}$$

$$= 75{,}000 \ \text{lb. in.}$$

Since the composite beam section was $10^1/_2$ in. wide the design moment per beam was 65,500 lb. in. The stresses in the 6 in. thick composite slab due to live load were

$$\pm \frac{65{,}600 \times 6}{10.5 \times 6^2} = \pm 1{,}040 \ \text{lb./in.}^2 .$$

Prestressing details

The four 0.2 in. diameter wires in the bottom flange were initially stressed to 72 tons/in.^{2} and had an eccentricity of 1.18 in.

Total prestressing force initially $= 4 \dfrac{\pi}{100} 72 \times 2{,}240 = 20{,}300 \ \text{lb.}$

If there is an assumed 15 % loss of stress, final force $= 17{,}300$ lb. The stress condition in the various fibres at various stages in construction is given below. All stresses are in lb./in.^{2}.

	Precast		In situ
	top fibre	bottom fibre	top fibre
Initial prestress	-466	1,571	—
Self weight	204	-108	—
Total initial stresses	-262	1,463	—
Total stresses after losses	-192	1,225	—
In situ concrete	343	-181	—
Total final stresses before live load applied	151	1,044	—
Live load stresses	780	$-1,040$	1,040
Stresses at design moment condition	931	4	1,040

Two untensioned 0.2 in. diameter high-tensile steel wires were placed in the top flange of the precast section to control the tensile stresses induced by post-tensioning and to facilitate handling.

Appendix II

Ultimate Strength of Composite Rectangular Beam

Bridge No. 1

The coefficients used in the ultimate load analysis are derived from the cube strength of the in situ concrete at the time of the tests to failure and from the relations given in a paper by HOGNESTAD, HANSON and McHENRY[1]).

Cube strength at time of tests to failure   = 10,050 lb./in.^{2}
Corresponding ultimate strain   = 0.0028
Average compressive stress in stress blocks   = 4,700 lb./in.^{2}
Position of centroid of compressive force   = 0.40 × depth to neutral axis

Strain in tensioned high-tensile steel
    before testing   = 0.0048

With the neutral axis at failure at a depth of 0.67 in. the total concrete force is

$$C = 0.67 \times 10.5 \times \frac{4,700}{2,240} = 14.75 \text{ tons.}$$

From the stress-strain curve for the prestressing steel the load per wire at the various strains was found to be:

at a strain of 0.0019:   0.92 tons
at a strain of 0.0244:   3.22 tons

Therefore total steel force = $4 \times 3,33 + 2 \times 0.92$
                         = 14.72 tons

Therefore the ultimate moment, M_{ult}, of the beam is
$12.88 \times 2,240 \ (5.36 - 0.268) + 1.84 \times 2,240 \ (1.125 - 0.268)$
$= 147,000 + 3,530 \text{ lb. in.}$
$\doteqdot 150,500 \text{ lb. in.}$

---

[1]) HOGNESTAD, E., HANSON, N. W., and McHENRY, D. Concrete stress distribution in ultimate strength design. Journal of the American Concrete Institute. Vol. 27, No. 4, December 1955, pp. 455—479.

Bridge No. 2

Using a similar analysis to that given above it was found that

$$M_1 = \text{ultimate moment/ft. transversely} = 167,000 \text{ lb. in.}$$
$$M_2 = \text{ultimate moment/ft. longitudinally} = 13,650 \text{ lb. in.}$$

Bridge No. 3

For this bridge it was found that

$$M_1 = 159,600 \text{ lb. in.}$$
$$M_2 = 13,580 \text{ lb. in.}$$

References

1. MORICE, P. B. and LITTLE, G., "The analysis of right bridge decks subjected to abnormal loading". London, Cement and Concrete Association. July 1956, pp. 43. Db. 11.
2. MORICE, P. B., LITTLE, G., and ROWE, R. E., "Design curves for the effects of concentrated loads on concrete bridges decks". London, Cement and Concrete Association. June 1956, pp. 24, Db. 11 a.
3. ROWE, R. E., "A load distribution theory for bridge slabs allowing for the effect of Poisson's ratio". Magazine of Concrete Research. Vol. 7, No. 20. July 1955, pp. 69—78. CACA Reprint No. 10.
4. LITTLE, G. and ROWE, R. E., "The effects of edge-stiffening and eccentric transverse prestress in bridges". London, Cement and Concrete Association, November 1957, pp. 20, Technical Report TRA/279.
5. ROWE. R. E., "The analysis and testing of a type of bridge suitable for medium right spans subjected to abnormal loading". London, Cement and Concrete Association, November 1958, Research Report No. 6.
6. BEST, B. C., and ROWE, R. E., "Abnormal loading on composite slab bridges (1). Tests on a bridge without transverse reinforcement". London, Cement and Concrete Association, 1958, Technical Report TRA/301.
7. BEST, B. C. and ROWE, R. E., "Abnormal loading of composite slab bridges (2). Tests on a bridge with some transverse reinforcement". London, Cement and Concrete Association, 1958, Technical Report TRA/307.
8. BEST, B. C. and ROWE, R. E., "Abnormal loading of composite slab bridges (3). Tests on a bridge with some transverse reinforcement". London, Cement and Concrete Association.
9. MORICE, P. B. and REYNOLDS, G. C., "The strength of simply supported slab bridges subjected to concentrated loads". Proceedings of a Symposium on the Strength of Concrete Structures. London, Cement and Concrete Association, 1958, pp. 557—572.
10. ROWE, R. E., "Load distribution in bridge slabs (with special reference to transverse bending moments determined from tests on three prestressed concrete slabs)". Magazine of Concrete Research. Vol. 9, No. 27, November 1957, pp. 151—160.
11. HOLLAND, A. D., "Prestressed units for short-span highway bridges. Proceedings of the Institution of Civil Engineers". Part II, Vol. 4, No. 2, June 1955, pp. 224—249. Discussion pp. 249—297.

Summary

The results obtained from tests on two small scale box section bridges and three composite slab bridges, comprising precast prestressed inverted T-beams, are presented and discussed in some detail.

In the case of the box-section types the results indicated that the normal methods of load distribution could be used to predict accurately the deflexions and stresses under abnormal loading conditions and that the methods of construction employed in the small scale model could be easily reproduced on site provided care was taken in the detailed design.

In the case of the composite slab bridges the tests have shown that distribution properties similar to those in an isotropic slab can be obtained without transverse prestress. The use of normal mild steel reinforcement based on an ultimate load analysis, with an appropriate load factor, does yield a satisfactory behaviour in both the elastic and ultimate load ranges. Even severe overloadings up to 1.5 × Working load do not have any significant effect on the distribution properties.

Résumé

L'auteur expose et discute en détail les résultats obtenus au cours d'essais effectués sur deux ponts à section en caisson et trois ponts à dalle composée comprenant des poutres préfabriquées précontraintes en T renversé; les ouvrages étaient réalisés à échelle réduite.

Les essais sur les ponts à section en caisson ont montré que, pour la détermination exacte des flexions et des contraintes sous l'effet des charges exceptionnelles, il est possible d'appliquer les méthodes habituelles de répartition des charges. Les dispositions constructives du modèle peuvent être aisément reproduites sur le chantier, pourvu que l'étude soit fait avec soin et d'une manière détaillée.

Les essais sur ponts à dalle composée ont permis de constater que sans précontrainte transversale, il est possible de réaliser des caractéristiques de répartition semblables a celles des dalles isotropes, lorsque l'on emploie une armature normale en acier doux, établie sur la base d'un calcul à la rupture, avec un coefficient de charge approprié, on obtient un comportement satisfaisant, aussi bien dans le domaine élastique qu'à la rupture. Même des surcharges importantes, atteignant jusqu'à 1,5 fois les charges normales de service, n'exercent aucune influence notable sur les caractéristiques de répartition.

Zusammenfassung

Der Verfasser setzt sich in dieser Abhandlung mit den Ergebnissen aus Versuchen an Kleinmodellen von zwei Kastenquerschnittbrücken auseinander, sowie drei zusammengesetzten Plattenbrücken aus vorfabrizierten, vorgespannten, umgekehrten T-Trägern die er bis in einige Details diskutiert.

Die Versuche an den Kastenquerschnitt-Typen ergaben, daß zur genauen Bestimmung der Durchbiegungen und Spannungen unter Ausnahmelast die üblichen Lastverteilungsmethoden angewandt werden können. Die bauliche Durchbildung des Modells kann auf dem Bauplatz leicht reproduziert werden, sofern die Details mit Sorgfalt geplant werden.

Bei den zusammengesetzten Plattenbrücken zeigten die Versuche, daß man ohne Quervorspannung ähnliche Verteilungseigenschaften erreichen kann wie bei isotropischen Platten. Wenn eine normale Flußstahlarmierung, beruhend auf einer Bruchlast-Analyse, mit angemessenem Belastungsfaktor verwendet wird, ergibt sich ein zufriedenstellendes Verhalten sowohl im elastischen als auch im Bruchzustand. Selbst starke Überlastungen, bis zu 1,5facher Gebrauchslast, bringen keinen nennenswerten Effekt auf die Verteilungseigenarten.